



Thiol-yne click crosslink hyaluronic acid/chitosan hydrogel for three-dimensional *in vitro* follicle development

Sureerat Khunmanee^{a,1}, Jungyoung Yoo^{b,c,1}, Jung Ryeol Lee^{c,d,**}, Jaewang Lee^{b,***}, Hansoo Park^{a,*}

^a Department of Integrative Engineering, Chung-Ang University, 221 Heukseok-Dong, Dongjak-Gu, Seoul, 06974, Republic of Korea

^b Department of Biomedical Laboratory Science, Eulji University, Gyeonggi-do, 13135, Republic of Korea

^c Department of Obstetrics and Gynecology, Seoul National University Bundang Hospital, Seongnam-si, Gyeonggi-do, 13620, Republic of Korea

^d Department of Obstetrics and Gynecology, Seoul National University College of Medicine, Seoul, 03080, Republic of Korea

ARTICLE INFO

Keywords:

Hyaluronic acid
Hydrogel
Follicle development
Oocyte maturation
Click crosslink

ABSTRACT

There is a great deal of potential for *in vitro* follicle growth to provide an alternative approach to fertility preservation. This strategy reduces the possibility of cancer cells re-exposure after transplantation, and it does not require hormone stimulation. Adopting a three-dimensional (3D) culture method helps preserve the architecture of the follicle and promotes the maturity of oocytes. In order to maintain follicle morphology, enhance the quality of mature oocytes, and facilitate meiotic spindle assembly, the current work aimed to develop the 3D *in vitro* preantral mouse follicle culture method. Thiolated chitosan-co-thiolated hyaluronic (CSHS) hydrogel was designed to evaluate the effects of biomaterials on ovarian follicle development. Isolated follicles from mouse ovaries were randomly divided into alginate (Alg) as a 3D control, thiolated hyaluronic acid (HASH), and CSHS groups. Single follicle was encapsulated in each hydrogel, and performed for 10 days and subsequently ovulated to retrieve mature oocytes on day 11. CSHS hydrogel promoted follicle survival and oocyte viability with maintained spherical morphology of follicle. Matured oocytes with normal appearance of meiotic spindle and chromosome alignment were higher in the CSHS group compared with those in the Alg and HASH groups. Furthermore, CSHS increased expression level of folliculogenesis genes (TGFβ-1, GDF-9) and endocrine-related genes (LHCGR, and FSHR). With various experimental setups and clinical applications, this platform could be applied as an alternative method to *in vitro* follicle culture with different experimental designs and clinical applications in the long-term period.

1. Introduction

There is a better understanding of the risk of premature ovarian failure from radiation or chemotherapy and the possibility of preserving fertility prior to administering the medication, which improves survival rates for young women diagnosed with cancer and other life-threatening diseases [1]. Oocyte and embryo cryopreservation, the most successful fertility preservation strategies, require a delay in cancer treatment for hormone stimulation to harvest mature oocytes, which may not be achievable for patients with aggressive cancers [2,3]. Hormone

stimulation is not such a solution for prepubescent girls, and ovarian tissue cryopreservation has the risk of reintroducing cancer cells into the patient [4].

An alternative fertility preservation option could be provided by *in vitro* follicle development [5]. This method does not require hormone stimulation and may minimize the chances of cancer cells re-exposure after transplantation [6]. Many oocytes could be retrieved whether spontaneously degenerating follicles were cultured *in vitro*, and women's reproductive ability could be restored by assisted reproductive technology [7,8]. Furthermore, *in vitro* culture of preantral follicles

* Corresponding author.

** Corresponding author.

*** Corresponding author.

E-mail addresses: sureeratkhunmanee@gmail.com (S. Khunmanee), malt392@naver.com (J. Yoo), leejrmd@snu.ac.kr (J.R. Lee), wangjaes@gmail.com (J. Lee), heyshoo@cau.ac.kr (H. Park).

¹ These authors contributed equally to this work.

<https://doi.org/10.1016/j.mtbio.2023.100867>

Received 11 July 2023; Received in revised form 9 November 2023; Accepted 14 November 2023

Available online 17 November 2023

2590-0064/© 2023 The Authors. Published by Elsevier Ltd. This is an open access article under the CC BY-NC-ND license (<http://creativecommons.org/licenses/by-nc-nd/4.0/>).

could assist in the preservation of the genetic profile of exotic species or animals with desirable traits [9]. Several *in vitro* follicle culture techniques have been actively studied and successfully supported ovarian follicles' growth and maturation in mice and several large mammalian species such as bovine, porcine, dog, chicken, and humans [9–15]. It is challenging to maintain the complex three-dimensional (3D) architecture of the follicle in two-dimensional (2D) culture environments, as well as the complex interactions between somatic cell components and the oocyte that are necessary to achieve cytoplasmic and nuclear maturation [16,17]. In addition, follicle flattening disrupts cell-to-cell communication, and as granulosa cells proliferate, they adhere to culture surfaces and rupture the basal membrane [18]. Data indicate that the oocyte's gap junctions and surrounding granulosa cells are critical for sharing paracrine factors and transporting specific amino acids to the oocyte [19].

The creation of 3D culture systems that imitate the *in vivo* environment of follicles has been the subject of extensive investigation [16,20]. Hydrogels have been used to transplant ovarian tissue or isolate follicles [21]. The 3D architecture of hydrogels could physically support the growth of follicles, maintain the follicular architecture and support the communication between follicular cells, and allow the expansion of early-stage follicles [21–23].

According to hydrogel properties, several natural and synthetic polymers, such as alginate (Alg), collagen, Matrigel, agarose, and polyethylene glycol (PEG), have been reported as bioactive materials to evaluate 3D culture systems for follicle development [24–28]. Among these, Alg is the most widely used biomaterial because it has shown favorable results with ovarian follicles. However, poor oocyte development resulting in abnormal spindle morphology and chromosome obtained from the Alg culture system makes it challenging to create a systematic approach for follicle culture improvement. Moreover, Alg lyase is required to degrade Alg to acquire developed culture follicles; however, this treatment damages granulosa and theca cells in ovarian follicles [29,30].

Hyaluronic acid (HA) is a naturally occurring biopolymer found in practically all mammalian tissues as part of the extracellular matrix (ECM) [31]. Because of its biocompatibility, biodegradability, and high water absorption capacity, HA has been widely used in various biomedical applications [25,32,33]. The application of a tyramine-based HA hydrogel to cultivate enzymatically extracted pre-antral mouse follicles was described by Desai et al. [34]. HA hydrogel is used in combination with extracellular matrix (ECM-HA) for the *in vitro* culture of ovarian follicles. In addition, hyaluronic acid-alginate (HAA) hydrogel and ovarian cells (OCs) were used to culture mouse ovarian follicles. A higher number of oocytes in the HAA-encapsulated follicles resumed meiosis greater than in Alg-encapsulated follicles [35].

Chitosan (CS) is composed of glucosamine and N-acetyl glucosamine coupled in a β structure employed in various biomedical applications [36]. The hydrogels based on chitosan have attracted much attention since this biopolymer is degraded by lysozyme in humans. CS hydrogels were employed to support follicle growth and maturation, and it was observed that the number of MII oocytes was higher in the 1% CS group compared to the 1% Alg group [37].

Beta-cyclodextrin (β -CD) is a cyclic oligosaccharide with a hydrophilic surface and stable hydrophobic core that can be modified and used to increase the cross-link density of gels. Additionally, β -CD has a conical hollow structure that allows small molecules to form host-guest complexes, and it does not change the overall hydrophilicity of the hydrogel matrix [38,39].

Thiolated polymers have been extensively researched for their many properties. These thiol groups are useful for building 3D hydrophilic networks by enabling cross-linking via disulfide bonds within their structure. Despite the simplicity of disulfide-bonded hydrogel networks, they have drawbacks, such as difficulty regulating the reaction and long gelation durations [40–42]. Thiol-ene reactions came into use to cross-link thiomers to alkenes in order to form stable hydrogels. They are

considered “clickable” because of their high efficiency and selectivity. Thiol-ene click reactions often display rapid reaction kinetics without the need for severe reaction conditions, and processes typically demonstrate excellent conversion yields. The ability of thiol-ene to occur selectively in the presence of other functional groups minimizes unfavorable side effects. Moreover, nucleophilic thiol-ene reactions are preferred over UV-initiated reactions in thiol-ene cross-linking, which employ a photo-initiator. UV-initiated reactions can be cytotoxic due to the release of free radicals.

In this research, we aimed to develop 3D *in vitro* pre-antral mouse follicle culture platforms. The goal was to create biomaterials that maintain structural integrity, enable hormone secretion and transport, facilitate nutrition, enhance matured oocyte quality, and promote meiotic spindle assembly. To achieve this, we emphasized the employment of various types of crosslinked hydrogels, including Schiff-base, disulfide, ionic interaction, and thiol-ene crosslinks for *in vitro* follicle culture. The investigation was the first fabrication of different types of hydrogel. HA was functionalized with thiol groups, resulting in a disulfide crosslinked thiolated hyaluronic acid (HASH). Then, we combined HASH with thiolated chitosan (CSH) through thiol-ene crosslinking with alkylated β -cyclodextrins (Alkyl- β -CD) to synthesize thiolated chitosan-co-thiolated hyaluronic (CSHS) hydrogel, Fig. 1. Third, the Schiff-based crosslink hydrogel based on HA and gelatin was fabricated. Finally, Alg crosslinked with CaCl_2 through ionic interaction was performed and utilized as a 3D control group for follicle culture. Through their investigations, the study aimed to provide valuable insights into the use of crosslinked hydrogels as a platform to provide an optimal microenvironment and enhance follicle development *in vitro*. It is important to note that, to the best of our knowledge, there have been no previous reports on the comparison of *in vitro* follicle growth and oocyte maturation using various types of crosslinked hydrogel systems. Moreover, *in vitro* follicle growth and oocyte maturation in CSHS hydrogel culture system have never been reported before, as well as lack of adequate studies regarding the *in vitro* culture of an isolated follicle in a combination of bioactive materials and the poor oocyte quality to resume meiotic competence retrieved from Alg culture system need to be further improved.

2. Materials and methods

2.1. Materials

HA (Mw = 1,000,000 Da) was obtained from CD bioparticles. 1-ethyl-3-(3-dimethylaminopropyl) carbodiimide hydrochloride (EDC, 99%), N-hydroxysuccinimide (NHS, 99%), cysteamine hydrochloride (CSA.HCl, 99%), dithiothreitol (DTT, 99%), 5, 5'-dithiobis-(2-nitrobenzoic acid) (DTNB, 99%), and L-cysteine ethyl ester hydrochloride (98%) were purchased from Sigma-Aldrich (MO, US). Phosphate-buffered saline (PBS, 0.0067 M) was purchased from Thermo Fisher Scientific Corporation (USA). Acetone was bought from Daejung. CS medium molecular weight, deacetylation $\geq 75\%$, 5' dithiobis(2-nitrobenzoic acid) ($\geq 8\%$), N,N-dimethylacetamide, L-cysteine, sodium acetate, 4-(Dimethylamino)pyridine (DMAP) reagentplus $\geq 99\%$, β -CD $\geq 97\%$, dimethylfuran (DMF), and N, N'-dicyclohexylcarbodiimide (DCC) $\geq 99\%$ were also obtained from Sigma-Aldrich (MO, US).

For follicle culture, α -minimum essential medium glutamax (α -MEM; Gibco, Paisley, UK) containing 5% Fetal bovine serum (FBS), 1% penicillin-streptomycin (PS, Sigma-Aldrich, MO, US), 1% ITS (5 mg/mL insulin, 5 mg/mL transferrin, and 5 ng/mL selenium; Sigma-Aldrich, MO, US), and 10 mIU/mL of recombinant human follicle-stimulating hormone (FSH; Merk-Serono, Darmstadt, Germany). Each follicle was cultured in a 96-well plate (SPL Life Science, Pocheon, Korea). Epidural growth factor and human chorionic gonadotropin were respectively purchased from Sigma-aldrich and Merck-Serono.

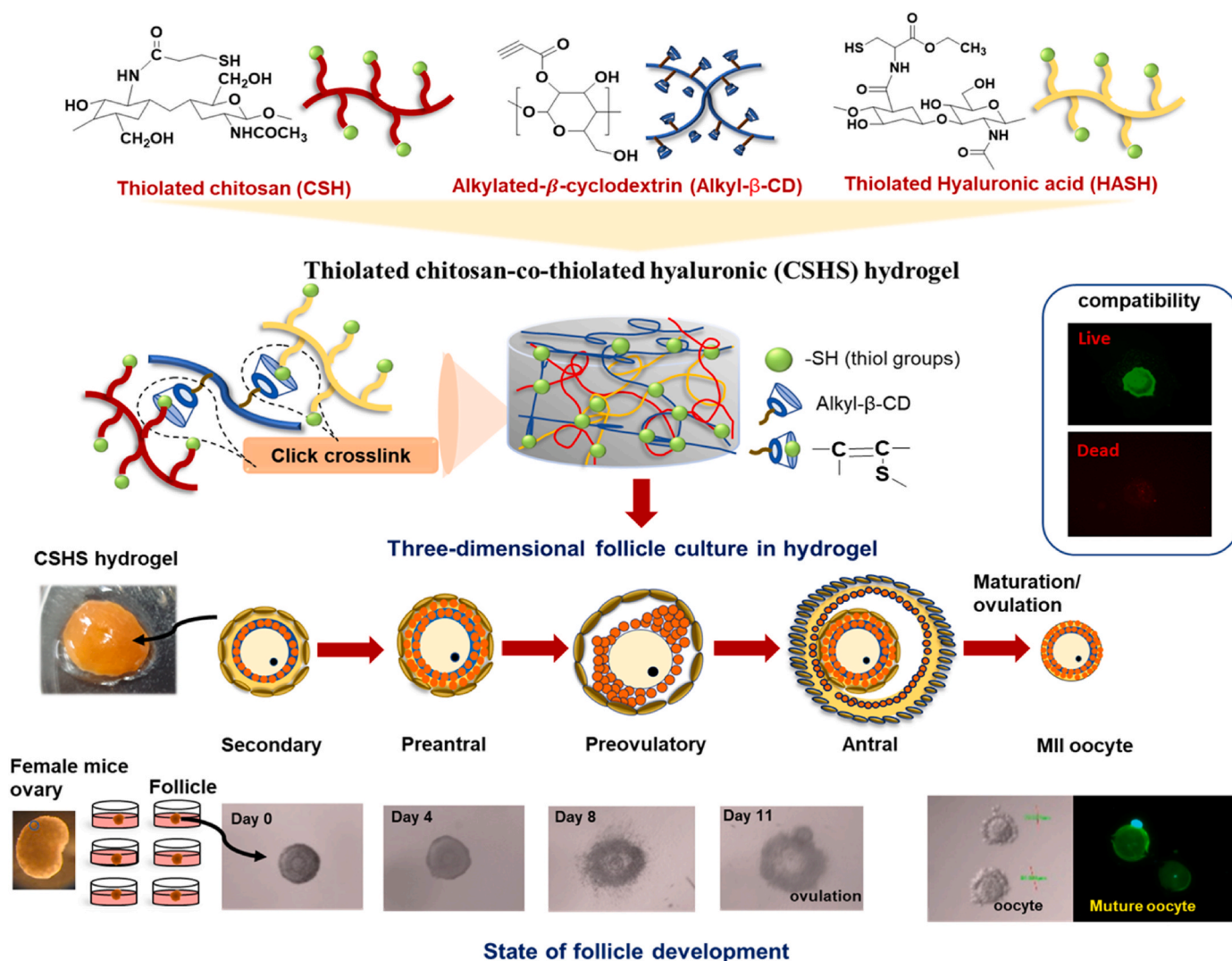


Fig. 1. A schematic illustration depicting the morphology of ovarian follicles at various developmental stages, the process of follicle isolation from a mouse ovary, and their subsequent encapsulation in thiolated chitosan-co-thiolated hyaluronic acid (CSHS) hydrogel.

2.2. Synthesis of thiolated hyaluronic acid (HASH)

HASH was synthesized following a modified method according to the process described by Bian et al. [40]. HA 0.4 g was dissolved thoroughly in 400 mL deionized water. Next, EDC (0.44 g) and NHS (0.28 g) were dissolved thoroughly in the HA solution by stirring at room temperature for 30 min. Subsequently, L-cysteine ethyl ester hydrochloride (600 mg) was added and continuously stirred under an N_2 atmosphere. The pH of the mixture solution was adjusted to 4.75 by adding 1.0 M NaOH. Then, 800 mg DTT was added and continuously stirred for 3 h. Finally, the solution was transferred to a dialysis tubing and dialyzed (MWCO 12,000–14,000, Spectra/Por membrane) exhaustively against 100 mM NaCl for 72 h, after which the solution was lyophilized to yield the HASH white sponge.

2.3. Synthesis of thiolated chitosan (CSH)

One gram of CS powder was dissolved in 100 mL 1% acetic acid solution. Then, EDC (2.5 g) was mixed by stirring for 30 min, and 2.5 mL of mercaptopropionic acid was added to the solution dropwise. The reaction was continued for 24 h under an N_2 atmosphere. After that, the reacted solution was dialyzed (MWCO 12,000–14,000, Spectra/Por membrane) exhaustively against double-distilled water for 3 days,

refreshed twice daily, and lyophilized to obtain the light-yellow sponge CSH.

2.4. Synthesis of alkylated β -cyclodextrins (alkyl- β -CD)

β -CD (1.135 g) was mixed with 45 mL DMF under an N_2 atmosphere. The mixture was dissolved entirely and 0.124 g of DMAP and 2.58 mL of propionic acid (98%) were added under continuous stirring for 15 min. DCC (2.88 g) was dissolved in 5 mL DMF and slowly added to the solution dropwise. The reaction continued for 24 h at 25 °C and stopped by adding 3 mL of double-distilled water. Then, the solution was filtered three times to remove 1,3-dicyclohexylurea (DCU), resulting in a clear brown solution. The clear brown solution was added dropwise slowly in cold acetone for precipitation, filtered using a sand core filter, and further purified by washing with acetone three times. The final product was dissolved in deionized water and freeze-dried by lyophilization at -80 °C. The brown powder was acquired and stored in a refrigerator at -20 °C.

2.5. Characterization of HASH, CSH, and alkyl- β -CD

Fourier transform infrared (FTIR) analysis of HASH, CSH, and alkyl- β -CD was performed to confirm the expected pendant functionalities.

Elemental analysis of the CSHS hydrogel surface was performed using X-Ray Photoelectron Spectroscopy XPS (K-alpha+, Thermo Fisher Scientific, Waltham, MA, USA) equipped with a spot area (on a 90° sample) of 400 μm and a monochromatic Al Kα X-ray source (200.0 eV). Each sample was cut into a circle with 1.0 cm diameter, and C1s, O1s, S2, and N1s were examined. The determination of free thiol content in HASH and CSH was conducted using Ellman's method. To summarize the procedure, HASH or CSH samples were mixed with deionized water, and a 0.2 M stock solution of DTNB was dissolved in tris buffer. The mixture was incubated at room temperature for 15 min, and the total free thiol group content in the sample was determined by measuring the maximum absorbance at 412 nm. A standard solution of L-cysteine was utilized for calibration (refer to Fig. S1).

2.6. Fabrication of HASH hydrogel

The HASH solution could crosslink automatically to form the hydrogel through the oxidation reaction of free thiol groups to form a disulfide bond. HASH polymer concentration 0.5% and 1% were dissolved in water (~pH 3.5), and the pH of the solution was regulated to 7.4 by adding 0.1 M NaOH. The freshly prepared HASH solution was immediately injected into a glass tube before exposure to air at room temperature.

2.7. Fabrication of CSHS hydrogel

The CSH solution with 0.5% and 1% concentrations were prepared. Alkyl-β-CD solution was prepared at a concentration of 0.125%. CSH solution and alkyl-β-CD were mixed at a volume ratio of 1:0.5 with adjusted pH to 7.4, and the hydrogel solution was transferred to a well, and subsequently, the HASH solution was added to form CSHS hydrogel (CSH:HASH = 1:1), Table S1.

2.8. Hydrogel morphology

Cross-section morphology of the hydrogels was observed using a scanning electron microscope (SEM; S-3400N, Hitachi, Tokyo, Japan). Freeze-dried hydrogel samples were further sputter-coated to observe the morphology and interior microstructure. All micrographs were products of secondary electron imaging and used to evaluate the surface morphology at different magnifications using an accelerating voltage of 5 kV.

2.9. Swelling measurement

Swelling studies of the swollen hydrogels were conducted gravimetrically. The temperature was set at 37 °C, and the pH was maintained at 7.4 using PBS. Hydrogel samples were taken from the buffer solution and weighed after removing the excess water on the surfaces with filter paper at predetermined time intervals. The equilibrium swelling was determined as equilibrium swelling (%) = $[(W_s - W_i)/W_i \times 100]$, where W_i is the weight of the initial hydrogel, and W_s is the equilibrium weight of the swollen hydrogel.

2.10. Rheological characterization of hydrogels

The viscoelastic behavior of the hydrogel was evaluated using a rheometer (Model Kinexus lab rheometer (Malvern)) with parallel plate geometry and oscillation frequency sweep tests. Briefly, 0.5% HASH and 0.5% CSHS were prepared to form hydrogel constructs. The hydrogels were placed on a parallel plate at 25 °C. A constant amplitude ($\gamma = 1\%$) was applied to the hydrogel at a frequency between 1 and 10 rad s⁻¹ and a gap size of 5 mm. The storage modulus (G') represents the elastic properties of materials.

2.11. Animals and ovarian follicle isolation

This study used 14-days-old Institute of Cancer Research (ICR) female mice purchased from OrientBio Inc. (Seongnam, Korea). All experimental animal procedures were performed in a pathogen-free laboratory (Ji-Seok-Yeong Biomedical Research Institute) and approved by the IACUC (Institutional Animal Care and Use Committee, IACUC number: BA-2007-299-059) of the Seoul National University Bundang Hospital. Euthanization was performed by cervical dislocation for ovarian tissue sampling. Ovaries were collected in an L-15 medium and mechanically isolated using fine needles in FBS-supplemented medium on a 60-mm culture dish (Nunc, Thermo Fisher Scientific, MA, USA). Among isolated follicles with bright colors of oocytes and granulosa cells and well intact cells around the oocytes, only those with a diameter of 120–150 μm in diameter, considered healthy secondary follicles, were selected for culture. The follicles were randomly divided into three groups: 3D control as 0.5% Alg, 0.5% HASH, and 0.5% CSHS *in vitro* culture. This experiment was repeated three times.

2.12. Follicle encapsulated in hydrogels

2.12.1. Follicle encapsulated in Alg

Single cultures were performed to track follicle growth. The isolated follicles were washed with 0.5% Alg solution to remove the remnant of the medium and then encapsulated into a 5 μL Alg-follicle gel with droplet shape in the crosslink solution. The rapidly encapsulated follicular Alg hydrogel was incubated in a pre-warmed (37 °C) 100 μL culture medium. On day 10 of culture, Alg lyase (Sigma-Aldrich, MO, US) was treated for follicle harvest and washed several times with fresh medium [43,44].

2.12.2. Follicle encapsulated in HASH

In the 0.5% and 1% HASH groups, 5 μL of the HASH solution was dropped in a 96-well plate, and a follicle was added to each well. HASH-containing follicle was crosslinked by increasing the pH to 7–8 with 0.1% NaOH for 15 min; then, 100 μL of culture medium was added.

2.12.3. Follicle encapsulated in CSHS

In the 0.5% and 1% CSHS groups, 2.5 μL of CSH was added to a 96-well plate, and 0.125% alkyl-β-CD solution was mixed at pH 7.4 to crosslink. Then, 2.5 μL HA-SH solution was added to the hydrogel, followed by a single follicle immediately in the hydrogel. The follicle encapsulated in the hydrogel was further crosslinked for 10 min; then, 100 μL of culture medium was added.

2.13. In vitro follicle culture and conditions

The culture medium used for *in vitro* follicle culture was 100 μL of α-minimum essential medium glutamax (α-MEM; Gibco, Paisley, UK) containing 5% FBS, 1% penicillin–streptomycin (PS, Sigma-Aldrich, MO, US), 1% ITS (5 mg/mL insulin, 5 mg/mL transferrin, and 5 ng/mL selenium; Sigma-Aldrich, MO, US), and 10 mIU/mL of recombinant human follicle-stimulating hormone (FSH; Merk-Sereno, Darmstadt, Germany). Each follicle was cultured in a 96-well plate (SPL Life Science, Pocheon, Korea). All follicles in 3D control (0.5% Alg), 0.5% HASH, and 0.5% CSHS groups were matured for 11 days, and on days 0, 4, 8, and 10, follicle observation and diameter measurements were performed to confirm the follicle growth or survival. Dead follicles were determined based on criteria, such as if the follicle contains dead or absent oocytes, if the oocyte was no longer surrounded by granulosa cells, if disintegrated granulosa cells had a dark color, or if there were no changes in diameter [45]. Half the culture medium was removed and refreshed on days 4, 8, and 10. On day 10 of maturation, half of the culture medium was removed and refreshed with an ovulation induction medium containing 5 ng/mL epithelium growth factor (Sigma-Aldrich) and 1.5 IU/mL hCG (Merck, Serono, Italy) in culture medium. Then, 18 h

later, the ovulated cumulus-oocyte-complexes were treated with $1 \times$ hyaluronidase (Sigma-Aldrich) to separate the cumulus cells from the oocyte. Finally, after oocyte observation and diameter measurement, oocytes were fixed with 4% paraformaldehyde (PFA) for further analysis [46,47].

2.14. Immunocytochemistry

The chromosome and meiotic spindle *in vivo* or *in vitro* ovulated oocytes were localized to evaluate meiotic maturation [48]. For the *in vivo* control, six-week-old female ICR mice were superovulated with 7.5 IU pregnant mare serum gonadotropin (Prospec, Israel) and 7.5 IU human chorionic gonadotropin (hCG; Sigma-Aldrich, USA) with a 48-h interval. Then, oocytes within the polar body thought to be in MII were retrieved for further staining. Oocytes were frozen in 4% PFA for 30 min before being permeabilized for 15 min in DPBS with 0.1% Triton X-100 and 0.3% bovine serum albumin (BSA). The oocytes were then blocked for 1 h in a 3% BSA solution at room temperature. The oocytes were incubated with primary antibodies as 1:200 anti-alpha tubulin (Cell Signaling Technologies, USA) solution for 2 h at room temperature and incubated with fluorescein isothiocyanate (FITC)-conjugated secondary antibodies as 1:1000 Alexa 488 (Life Technologies, USA). Finally, oocytes were mounted with Vectorshield mounting solution (Vector Laboratories, Burlingame, USA) containing 4'-diamidino-2-phenylindole (DAPI, Sigma, MO, USA). Images were taken using an upright fluorescence microscope (Axio Imager M2, Carl Zeiss, Germany) at $400 \times$ magnification [49,50].

2.15. Gene expression and RNA extraction

After oocytes were obtained on the 11th day of culture, granulosa cells (GCs) attached to the plate were collected by pipetting into microtubes by a group. First, RNA was extracted using the RNeasy kit (Qiagen, Germany). Then, collected GCs were homogenized in the buffer using a grinder, and total RNAs were collected by centrifugation using the kit's filter following the manufacturer's protocol. The primers' cDNA sequences were constructed using the National Center for Biotechnology Information database, and all polymerase chain reaction (PCR) primers used are shown in Table S2. Real-time quantitative PCR was performed in triplicate, using Q-PCR Master mix SYBR Green with low ROX (Enzynomics, Daejeon, Korea). Cycling conditions were denaturing at 95°C for 5 s and extension at 58°C for 25 s for 40 cycles. The relative gene expression was calculated using the delta-delta CT ($2^{-\Delta\Delta\text{CT}}$) method. Finally, levels were normalized to Glyceraldehyde-3-phosphate dehydrogenase (GAPDH) amplification.

2.16. Statistical analysis

Statistical analyses were conducted using GraphPad Prism v.6.0 (GraphPad Software, CA, US). All experiments were performed using three independent biological replicates, and the data, except the meiotic competence, were analyzed using one-way ANOVA (analysis of variance), followed by Tukey's test.

2.17. Ethics statement and consent to participate

All experimental animal procedures were performed in a pathogen-free laboratory (Ji-Seok-Yeong Biomedical Research Institute) and approved by the IACUC (Institutional Animal Care and Use Committee, IACUC number: BA-2007-299-059) of the Seoul National University Bundang Hospital.

3. Results

3.1. Synthesis and characterization of HASH, CSH, and alkyl- β -CD

FTIR was used to confirm CSH, HASH, Alkyl- β -CD, and CSHS structures. The -OH stretching vibration of HASH was observed at $\sim 3380\text{ cm}^{-1}$. The peak at 2918 cm^{-1} was assigned to C-H stretching, whereas the peak at 1052 cm^{-1} was attributed to the C-O-C stretching vibration. The amide bond (N-C=O) was observed at a wavelength of 1660 cm^{-1} , whereas C=O was identified at 1440 cm^{-1} , Fig. 2a.

CSH was prepared using modified amine groups with thiol groups in acidic conditions. The -OH stretching vibration was observed at 3400 cm^{-1} , and the peak at 2930 cm^{-1} indicated C-H stretching. Furthermore, the peak at 1076 cm^{-1} was attributed to -C-O-C- stretching vibration. CS-SH has amide bonds of 1627 cm^{-1} (N-C=O) and 1528 cm^{-1} (N-C=O) (N-H). The additional weak peak of the S-H stretch was observed around $2000\text{--}2400\text{ cm}^{-1}$, Fig. 2b. HASH and CSH was further determined with Ellman's reagent, leading to a value of $9.08 \times 10^{-4}\text{ M}$ and $1.3 \times 10^{-3}\text{ M}$, (Fig. S1).

Alkyl- β -CD was obtained by reacting β -CD and propargyl acid. The antisymmetric stretching peak of CH_2 was identified at around 2920 cm^{-1} . The peaks at 1190 cm^{-1} and 1024 cm^{-1} are attributed to the C-O and C-O-C stretching vibrations. The peak around 700 cm^{-1} was the rocking vibration of $-\text{CH}_2$. Additionally, the peak appears at 2095 cm^{-1} and 1728 cm^{-1} , corresponding to $\text{C}\equiv\text{C}$ and $\text{C}=\text{O}$, respectively, Fig. 2c.

The FTIR spectra of CSHS confirm that crosslinking of CSH, Alkyl- β -CD and HASH were successful. Alkynyl groups ($\text{C}\equiv\text{C}$) were observed at 2100 cm^{-1} , and the peaks at 1034 cm^{-1} are attributed to the C-O-C stretching, which shows significant changes, Fig. 2d.

3.2. Hydrogel fabrication

HASH hydrogel was acquired by self-crosslinking via oxidization in the air of two thiol groups to form a disulfide bond at neutral or basic conditions. HASH solution at concentrations of 0.5% HASH and 1% HASH were prepared. The pH of the solution was adjusted to 7–8 by 0.1% NaOH, and gelation occurred within 10–15 min. Preparation of CSHS hydrogel was conducted via a Michael-type "thiol-yne" click reaction between -SH and alkynyl groups in alkyl- β -CD without additional chemical agents. HASH and CSHS hydrogels were further evaluated for swelling ratio, mechanical test, and microstructure because these properties significantly impact cell penetration, proliferation, and function in tissue engineering.

The XPS results (Fig. 2a, Fig. S2a) confirmed the CSHS hydrogel. The binding energy range was selected to detect carbon (C), nitrogen (N), oxygen (O) and sulfur (S). In particular, the location of the N signal is important as this indicates amide bonding CSH. The CSHS surface exhibited N peak at the N1s binding-energy sites from 396 to 408 eV. The C peak (281–295 eV) at the C1s binding energy related to (C-C), (C-O-C) and (O=C-C) groups. These results show that the XPS spectra of O1s was 531–533 eV (C-O and C=O). Furthermore, the S2p peak (161–168 eV) suggest that SH conjugation was successfully fabricated via chemical methods [51]. HASH and CSHS hydrogels were further evaluated for swelling ratio, mechanical test, and microstructure because these properties significantly impact cell penetration, proliferation, and function in tissue engineering [52,53].

3.3. Swelling ratio, elastic modulus, and hydrogel morphology

According to Fig. 3b, swelling ratio of HASH hydrogel increased sharply from 2 h to 4 h and then slightly increased and remained constant until 24 h (60%). CSHS and Alg hydrogels showed a slightly increased swelling ratio from 2 h to 8 h and remained constant until 24 h (12% and 8%, respectively). Additionally, 0.5% HASH exhibited much higher water uptake than 0.5% CSHS and 0.5% Alg, respectively.

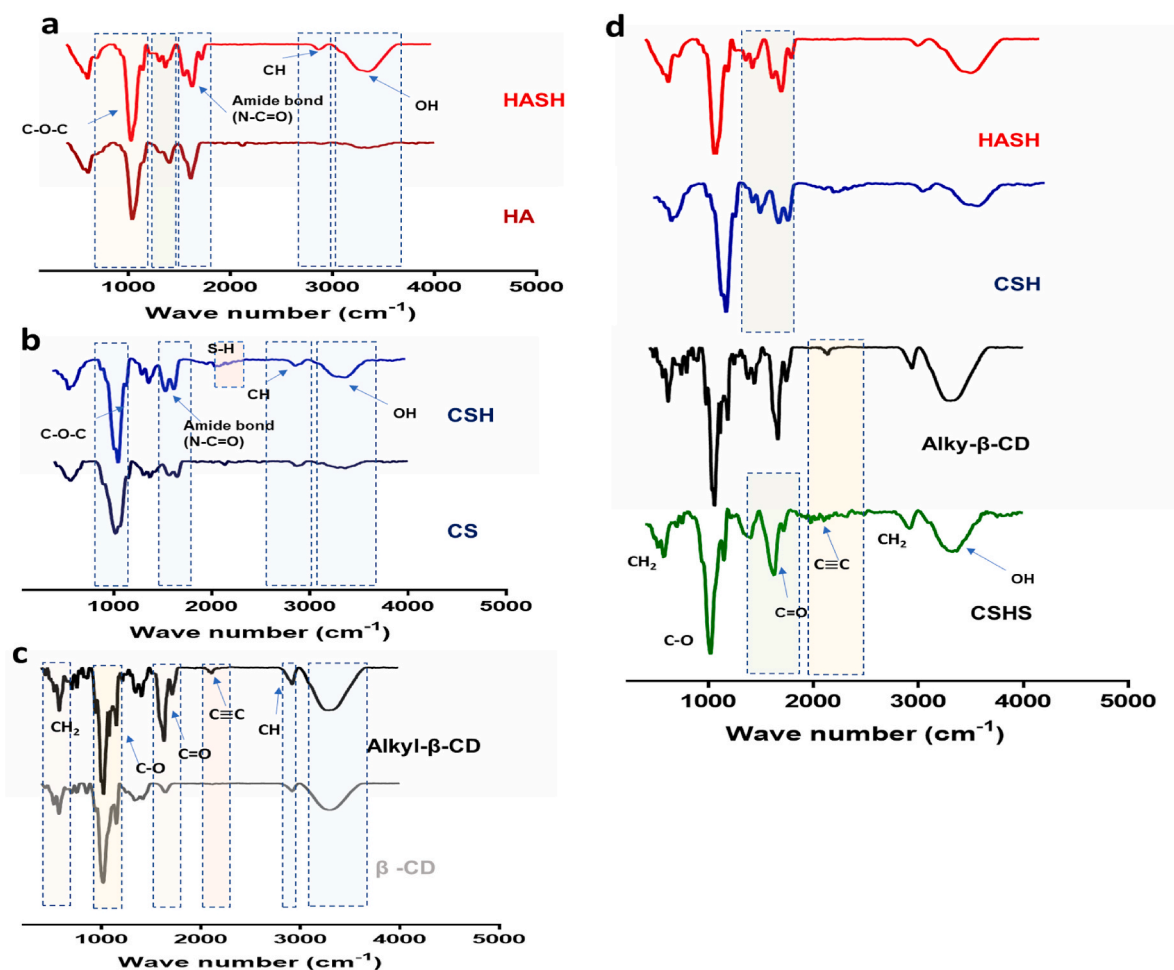


Fig. 2. FTIR spectra of (a) HA, HASH, (b) CS, CSH, (c) β -CD, Alkyl- β -CD, and (d) CSHS hydrogel.

Furthermore, the swelling ratio of 1 % HASH was lower than that of 0.5 % HASH. A similar outcome was discovered in the CSHS system. The swelling ratio of hydrogels could be attributed to the microstructure and hydrophilic nature of the scaffold. These results explain that the high hydrophilicity of HASH may also have contributed to the high swelling ratio and high degradation properties. The effect of Alkyl- β -CD concentration on CSHS hydrogel at concentration 0.5% was also evaluated on swelling ratio. Alkyl- β -CD at concentration 0.125% was selected to prepare CSHS hydrogel due to the greatest of swelling properties and low toxicity, Fig. S2b, Figs. S3a and S3b.

To observe the structure of the hydrogels, SEM images were taken as shown in Fig. 3c. SEM pictures of the lyophilized hydrogel before swelling showed an interconnected porous structure with pore sizes around 500–600 μm (0.5% and 1% HASH), and 250–300 μm (0.5% and 1% CSHS). The average pore size of scaffolds decreased by the increase in crosslink density. Additionally, CSHS and HASH showed homogeneously distributed porous structures; HASH showed larger pore sizes than CSHS, which is in good agreement with swelling experiments observed in these hydrogels. However, the 0.5% Alg hydrogel displayed an uneven and non-uniform porous structure, along with partially condensed filament-like regions. The swollen Alg hydrogel displayed nearly identical morphological characteristics before and after swelling, primarily due to the high mechanical properties of Alg, which resulted in a slower degradation rate. In contrast, post-swelling of the 0.5% and 1% HASH concentrations exhibited an open and irregular collapsed structure. Specifically, the network of the 0.5% HASH hydrogel tended to collapse and displayed a filament-like structure due to degradation, while a certain part of 1% HASH hydrogel still maintained porous

morphology. It's worth noting that the 0.5% and 1% CSHS hydrogels, after swelling, experienced a reduction in pore size, resulting in a shrunken state. Nevertheless, the CSHS hydrogel post-swelling retained a more porous structure when compared to the HASH hydrogel at corresponding concentrations.

Another crucial aspect of hydrogel culture system for follicle development is the mechanical properties of the hydrogel. Fig. 3d shows the G' of 0.5% HASH was 31 Pa which was lower than that of the 0.5% CSHS (85 Pa). It might be concluded that these hydrogels provided sufficient stiffness to maintain the 3D configuration of the follicle, and also provide for an increased follicle size due to oocyte growth, stromal cell proliferation, and antrum development. Consequently, several of parameters influence the overall transport properties of hydrogels employed for follicular encapsulation. Understanding these features is essential in the development of the follicle culture system.

3.4. Follicle development and morphology

The mouse ovaries were collected from 14-days-old mice and mechanically dissected using needle in puncture media, Fig. 4a. Morphologically intact preantral follicles were isolated (diameter: 100–120 μm), and randomly divided in to three groups: 0.5% Alg, 0.5% HASH and 0.5% CSHS. The follicles were encapsulated in hydrogel and cultured for 10 days. The follicular development stage could be assessed through morphological observation. The stage from follicular differentiation to antral follicle formation is important key for the release of polar body from mature follicular oocytes, Fig. 4b. Fig. 4c shows the morphological changes in follicle culture of 0.5% Alg, 0.5% HASH and 0.5% CSHS

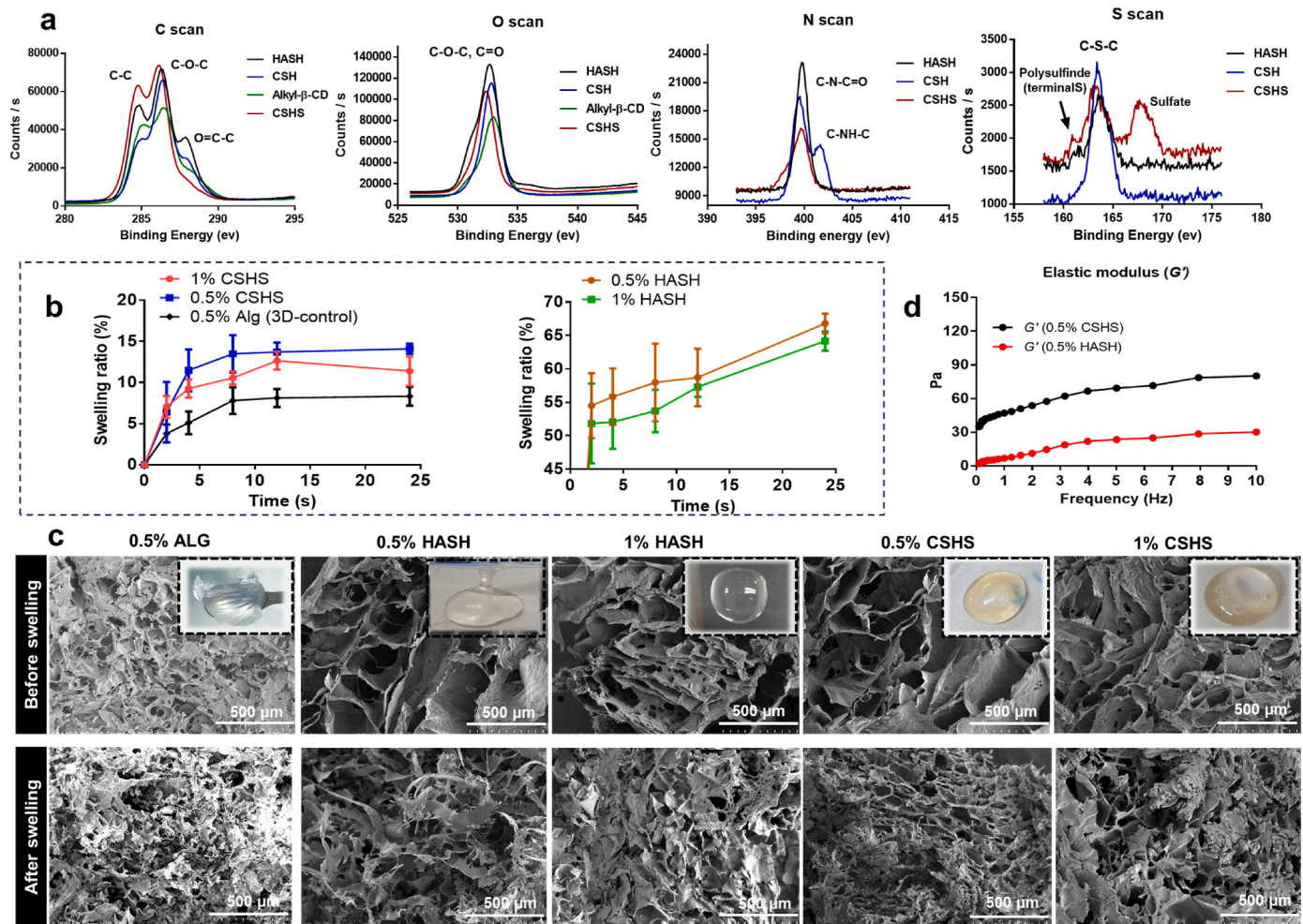


Fig. 3. X-ray photoelectron spectroscopy (XPS) results of CSHS hydrogel. BE: binding energy. XPS elemental composition analyses in the regions of N1s, C1s, O1s and S2p (a), percentage of the swelling ratio of hydrogel (b), SEM image comparing the microstructure of Alg, HASH, and CSHS hydrogels before and after swelling 7 days (Scale bar 500 μm) (c), and the G' of HASH, and CSHS hydrogels (d).

hydrogel for 11 days. Three hydrogel groups could support follicle growth and maintain their spheroidal follicle shape. On the 10th day of culture, follicle survival rates were not significantly different among 0.5% Alg, 0.5% HASH, and 0.5% CSHS (93.0%, 86.4%, and 85.7% respectively), Fig. 5a. Follicle diameter in the 0.5% Alg group was ~ 350 μm , smaller than 0.5% HASH (follicle diameter ~ 450 μm) and 0.5% CSHS hydrogel (follicle diameter ~ 400 μm), Fig. 5b. After ovulation on the 11th day, oocyte morphology, oocyte retrieval rate and viability were investigated, Fig. 5c and d. The 0.5% Alg, 0.5% HASH, and 0.5% CSHS groups showed oocyte percentage retrieval of 73.9% ($n = 46$), 61.9% ($n = 42$), and 69.7% ($n = 33$), respectively, Fig. 5d. The oocyte viability was not significantly different among the three hydrogel groups, with oocyte diameter in all groups being an average of 70 \sim 75 μm and oocyte viability $\sim 80\%$, Fig. 5c,e-h.

3.5. Evaluation of mature oocytes

In this study, oocytes quality produced from 0.5% Alg, 0.5% HASH, and 0.5% CSHS were measured for their ability to continue meiosis as shown in Fig. 6. Oocytes retrieved from 0.5% HASH showed significantly higher GV rate than 0.5% Alg (45.8%, $n = 24$ vs. 11.7%, $n = 34$). Additionally, there was no significant difference between 0.5% HASH and 0.5% CSHS. Furthermore, the percentage oocyte undergoing GVBD of 0.5% HASH was greater among three groups (28.6%, $n = 21$), but it was not significantly different from 0.5% CSHS (18.5%, $n = 27$) and

0.5% Alg (18.1%, $n = 22$). MII rate was significantly higher in 0.5% CSHS (29.1%, $n = 24$) than 0.5% Alg (8.8%, $n = 34$). However, a statistically significant difference was not observed comparing with 0.5% HASH (21.4%, $n = 14$).

In our study, the majority of MII oocytes with normal spindle morphology and chromosome alignment came from follicles encapsulated in 0.5% CSHS hydrogel (34.8%). On the other hand, the oocytes cultured in 0.5% HASH showed the lower percentage of normal spindle (25.0%), and 0.5% Alg exhibited the lowest normal spindle (20%), Table 1. This morphology was comparable to what was observed in MII oocytes produced by superovulation *in vivo*, Fig. 7. Interestingly, matured oocytes cultured from 0.5% Alg not only had a lower MII oocytes percentage, but the oocytes also had a higher proportion of abnormal oocytes (or dead)/GV/GVBD (64%) than 0.5% CSHS and 0.5% HASH (58.4% and 52.2%) respectively.

3.6. Gene expression analysis

The expressions of some genes involved in growth and differentiation of follicles, steroidogenesis, and apoptosis were assessed. Fig. 8 shows the relative expression levels, which were normalized against the level of GAPDH as an internal control. Transforming growth factor beta 1 (TGF- β 1) has been demonstrated to be expressed in mammalian ovarian cells and has a crucial role in the development of antral follicles and the metabolism of steroid hormones. Interestingly, it has been observed that

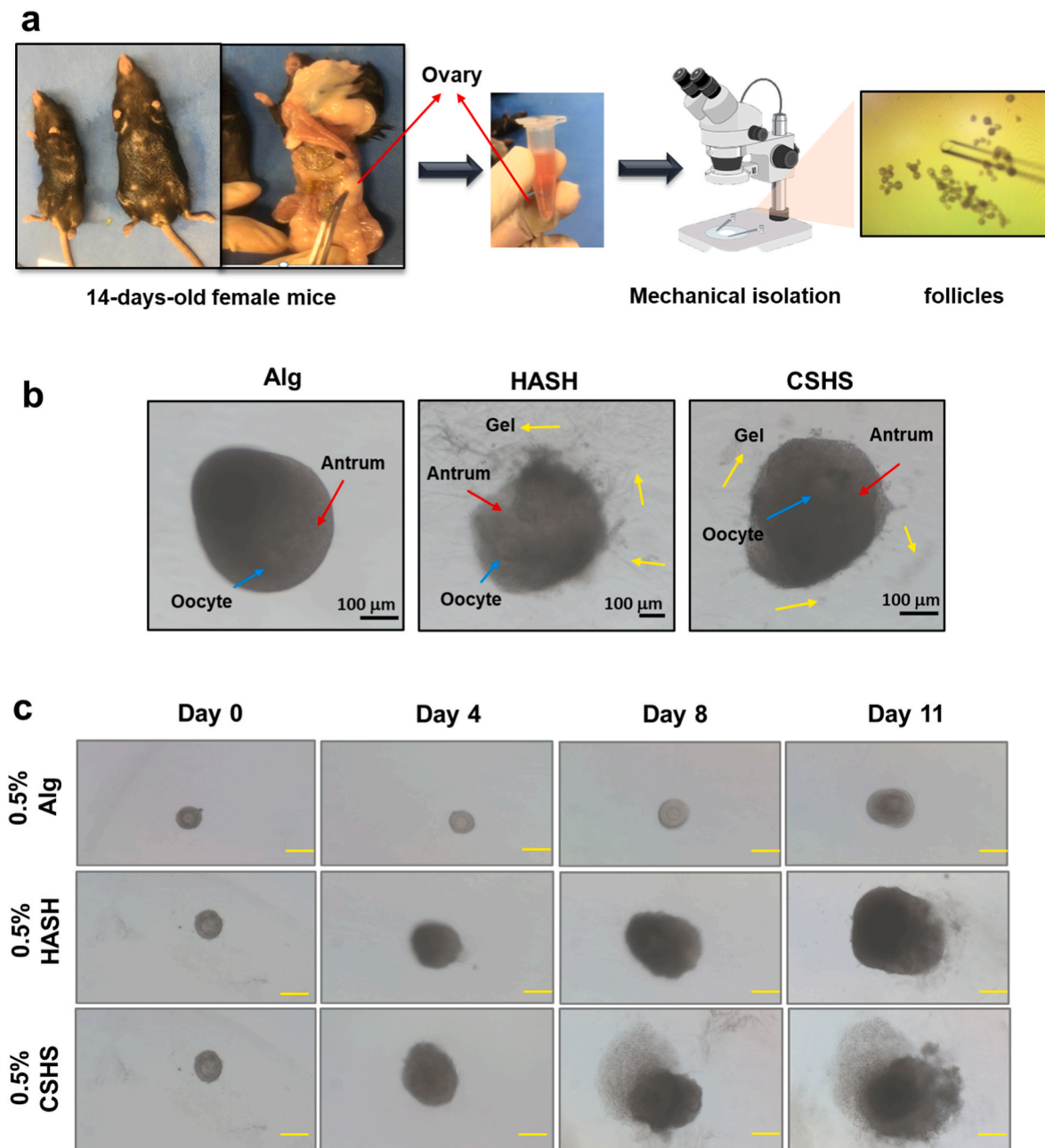


Fig. 4. Follicle isolation from mouse ovaries (a), a representative of antrum cavity (red arrows), oocytes (blue arrows), and hydrogels (yellow arrows) at day 8 of culture (b), and growth and morphological changes in preantral follicles cultured in 0.5% Alg, 0.5% HASH, and 0.5% CSHS (Scale bar 100 μ m, magnification 4 \times) (c). (For interpretation of the references to color in this figure legend, the reader is referred to the Web version of this article.)

TGF- β 1 had greater expression significantly in 0.5% CSHS than 0.5% Alg and 0.5% HASH, however there was no difference between 0.5% Alg and 0.5% HASH. All follicular stages contain the oocyte-secreted protein (GDF9). The expression of GDF9 was significantly higher in 0.5% CSHS compared to the 0.5% Alg and 0.5% HASH; however, there was no significant difference between the 0.5% Alg and 0.5% HASH.

The regulation of apoptosis genes involved B-cell lymphoma 2 (BCL2) as anti-apoptotic and BCL2 Associated X (BAX) as pro-apoptotic. These two genes in particular play an important role in various types of cells and are used in the examination of apoptosis in follicles and oocytes. There was a difference in the relative expression of BCL2 gene between 0.5% Alg with 0.5% HASH and 0.5% CSHS, but there was no such difference between the 0.5% HASH and 0.5% CSHS. Meanwhile, the expression of BAX was found to be over expressed in 0.5% CSHS, while the amount of BAX did not differ between 0.5% Alg and 0.5%

HASH. The follicles at the beginning of atresia may be the cause of the increased BCL2 expression in 0.5% CSHS.

The expression of Follicle Stimulating Hormone Receptor (FSHR) in developing follicles is crucial for proper ovulation and fertility because the FSH-FSHR interaction stimulates a series of intracellular signaling pathways that lead to the generation of steroid hormones, follicular maturation, and oogenesis. Interestingly, we discovered that 0.5% CSHS hydrogel considerably upregulated the expression of the FSHR gene when compared to 0.5% HASH and 0.5% Alg, respectively ($P < 0.05$). Luteinizing hormone/choriogonadotropin receptor (LHCGR) is another gonadotropin receptor that is expressed in mature follicles *in vivo* as they approach ovulation. In comparison to the 0.5% Alg group, our study found that the expression of LHCGR dramatically increased in the 0.5% CSHS and 0.5% HASH groups. Hence, in order to improve oocyte maturation, we hypothesized that 0.5% CSHS and 0.5% HASH might

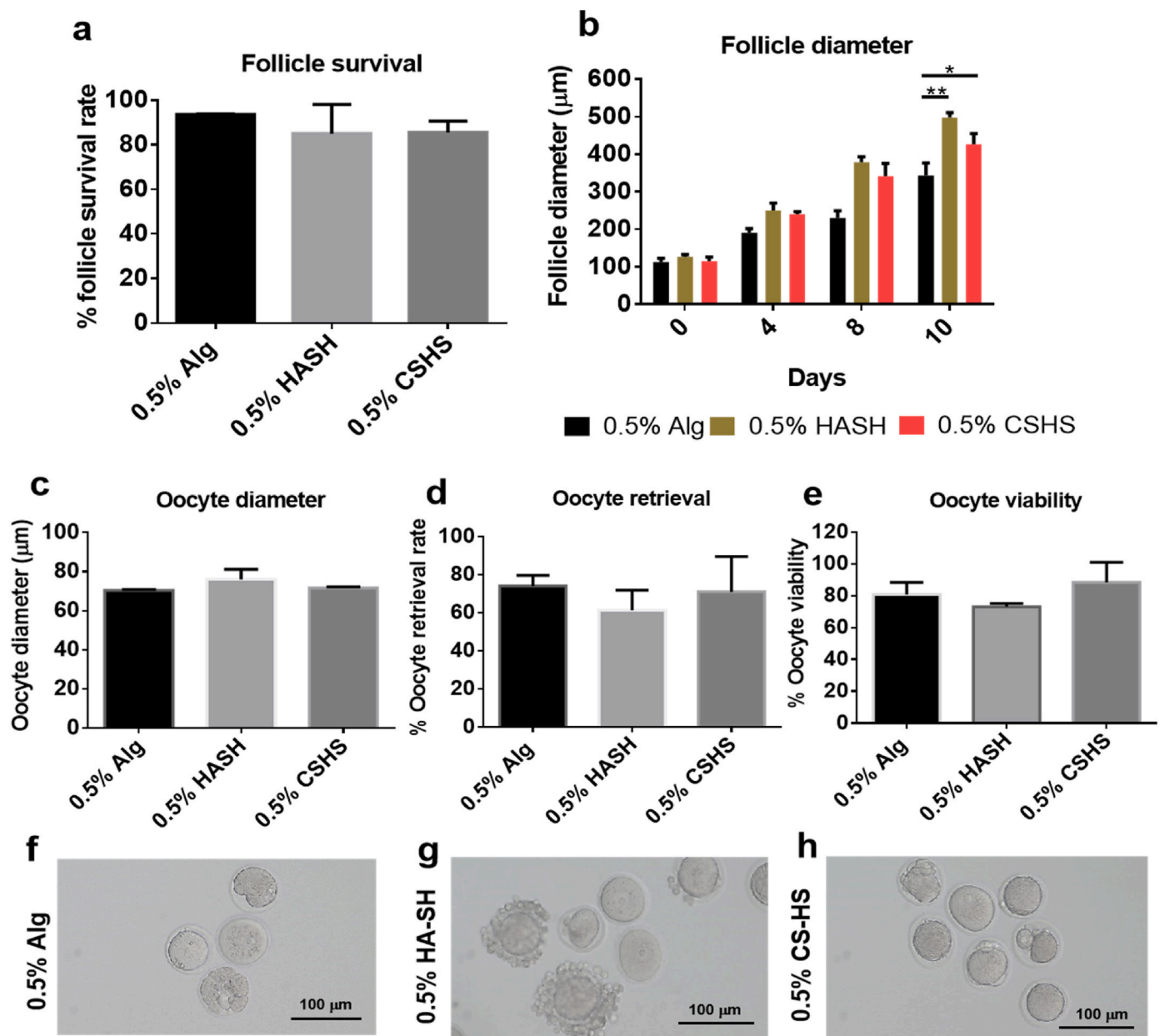


Fig. 5. Data represent follicle survival rate (a), diameters of surviving follicles on days 0, 4, 8, and 10 of culture (b), oocyte diameter (c), oocyte retrieval rate (d), oocyte viability (e), oocyte morphology on day 11 (f, g and h). Statistical analysis was performed by two-way analysis of variance (ANOVA) or Tukey's test. The results are expressed as the mean \pm standard deviation (SD; $n = 4$). * $p < 0.05$; ** $p < 0.01$; *** $p < 0.001$; **** $p < 0.0001$. The data represent three separate experiments.

upregulate LHCGR gene expression.

4. Discussion

Hydrogels are extensively employed in the field of tissue engineering, which develops materials and methods for repairing and replacing damaged or diseased tissue. In the area of follicle maturation, hydrogel can serve as a stroma that produces a cellular environment designed to provide the elements that stimulate maturation of ovarian follicles, but lacks the factors found in the native stroma that inhibit follicle maturation.

Characterizing the physical properties of hydrogel is essential to investigate the influence of the mechanical environment on cells created by an *in vitro* culture system. The equilibrium swelling ratio plays an essential role in maintaining the defined hydrogel structure and

retaining sufficient nutrient and water. The 3D architecture of the hydrogel's network is crucial for providing a permissive environment for follicle culture because it will regulate the rate at which nutrients and waste flow between the culture media and the encapsulated cell. The pore size is an important characteristic of the hydrogel architecture that is affected by polymer concentration. Any supplement in the culture media must diffuse into the hydrogel and then navigate to the encapsulated cells via the hydrogel's surface. The time it takes for a solute to proceed this route will be largely determined by the pore size and tortuosity. There may be considerable mass transfer limitations if the pore size is small in comparison to the diffusing molecules. In addition, the previous studies revealed that protein and oxygen can be transported through the hydrogel; however, the diffusion rate is impeded by Alg [54]. Another crucial aspect of hydrogel culture system for follicle development is the mechanical properties of the hydrogel. The hydrogel

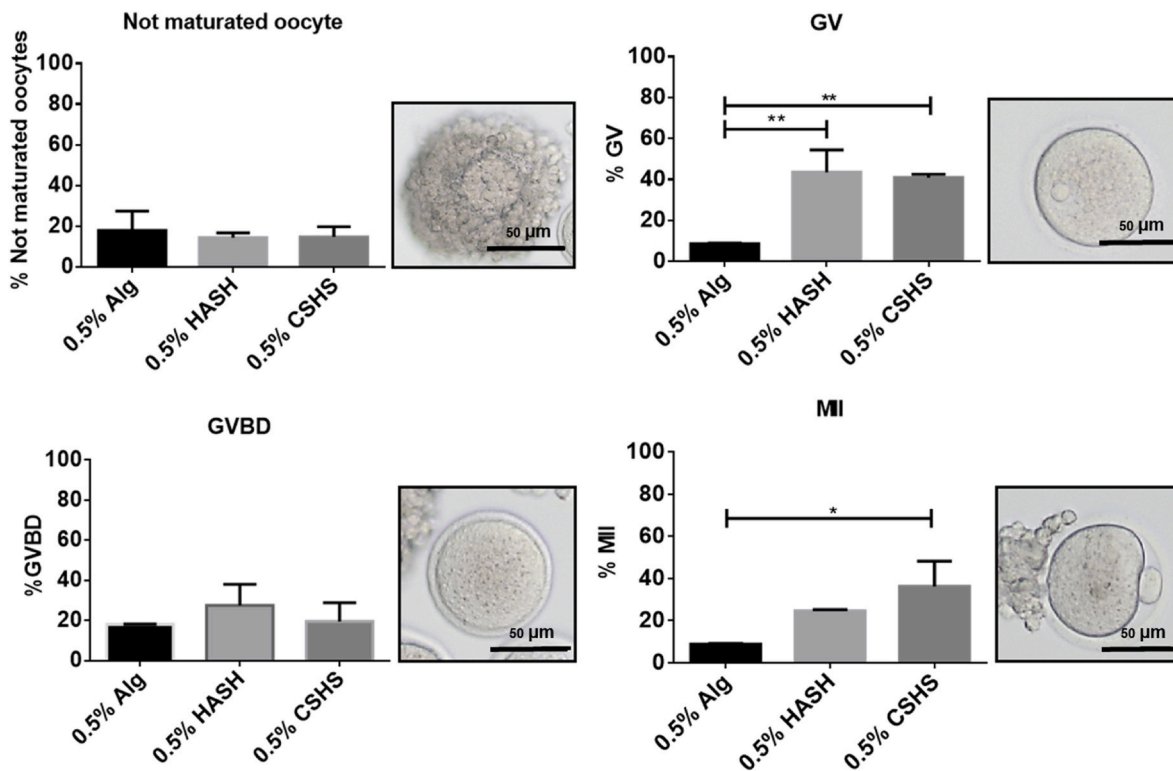


Fig. 6. Oocyte maturation under hydrogels; not matured oocyte, GV, GVBD, and MII. (Scale bar 50 μm, magnification 20×). Statistical analysis was performed by one-way analysis of variance (ANOVA) or Tukey’s test. The results are expressed as the mean ± standard deviation (SD; n = 4). **p* < 0.05; ***p* < 0.01; ****p* < 0.001; *****p* < 0.0001. The data represent three separate experiments.

Table 1

Percentage spindle normalities and spindle abnormalities of MII oocytes after maturation, obtained from culture in 0.5% Alg, 0.5% HASH, and 0.5% CSHS hydrogels.

Hydrogel	Metaphase II (MII)		GV/GVBD/abnormal oocytes
	Normal spindle	Abnormal spindle	
0.5% Alg	20.0% (5/25)	16.0% (4/25)	64.0% (16/25)
0.5% HASH	25.0% (6/24)	16.6% (4/24)	58.4% (14/24)
0.5% CSHS	34.8% (8/23)	13.0% (3/23)	52.2% (12/23)

must provide support to retain the follicle’s 3D architecture, but it must not restrict follicle growth. A previous study discovered extracellular matrix soft hydrogel (ES-hydrogel) was found to have a *G*’ that was much lower than that of Alg (1000 Pa), indicating that greater hormone exchange through a less stiff material may have contributed to the follicle development and oocyte maturation in the ES-hydrogel group [55]. An

another previous study found that a permissive environment might be defined as one with a storage modulus lower than 300 Pa [48]. West et al. demonstrated that decreased stiffness creates an environment that is more favorable for nutrition and hormone exchange [56].

In various studies, 3D *in vitro* follicle culture systems have been employed. The prerequisites for ideal culture conditions and *in vitro* follicle growth are still poorly understood. Hydrogels have been employed for various purposes, including regulating cell behavior, facilitating stem cell expansion and differentiation, and creating a suitable microenvironment for transplanting ovarian tissue or isolating follicles. Several synthetic and natural polymers have been used for *in vitro* follicle culture cultures. Considering the synthetic polymers, PEG is one of the most commonly tested materials for ovarian follicles culture [22]. PEG have suitable properties to apply for constructing an appropriate scaffold. It is basically synthetic and thus poor in biological features. Fewer oocytes were retrieved from PEG hydrogel [22,57]. Several prior studies have highlighted Alg as a promising natural material for successful 3D follicle culture. Woodruff’s research group showed that

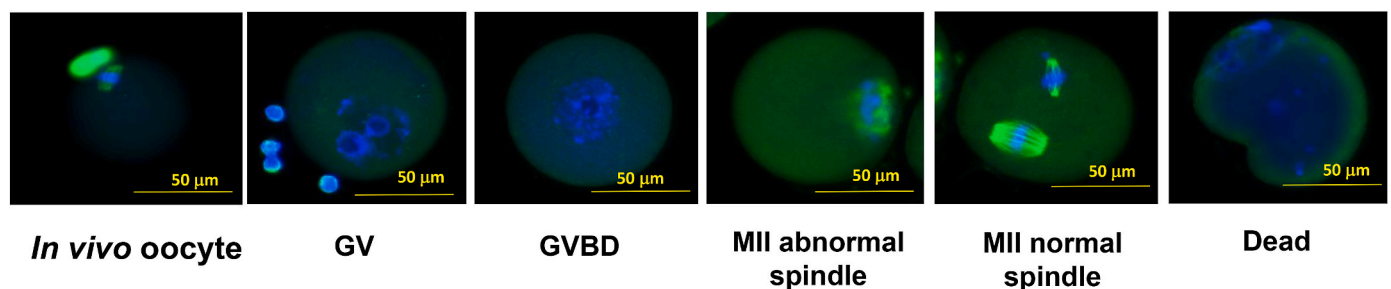


Fig. 7. Representative of meiotic spindle morphology and chromosome alignment with well-organized microtubule fibers (green) and tightly aligned chromosomes (blue) (scale bar: 50 μm, magnification 20×). (For interpretation of the references to color in this figure legend, the reader is referred to the Web version of this article.)

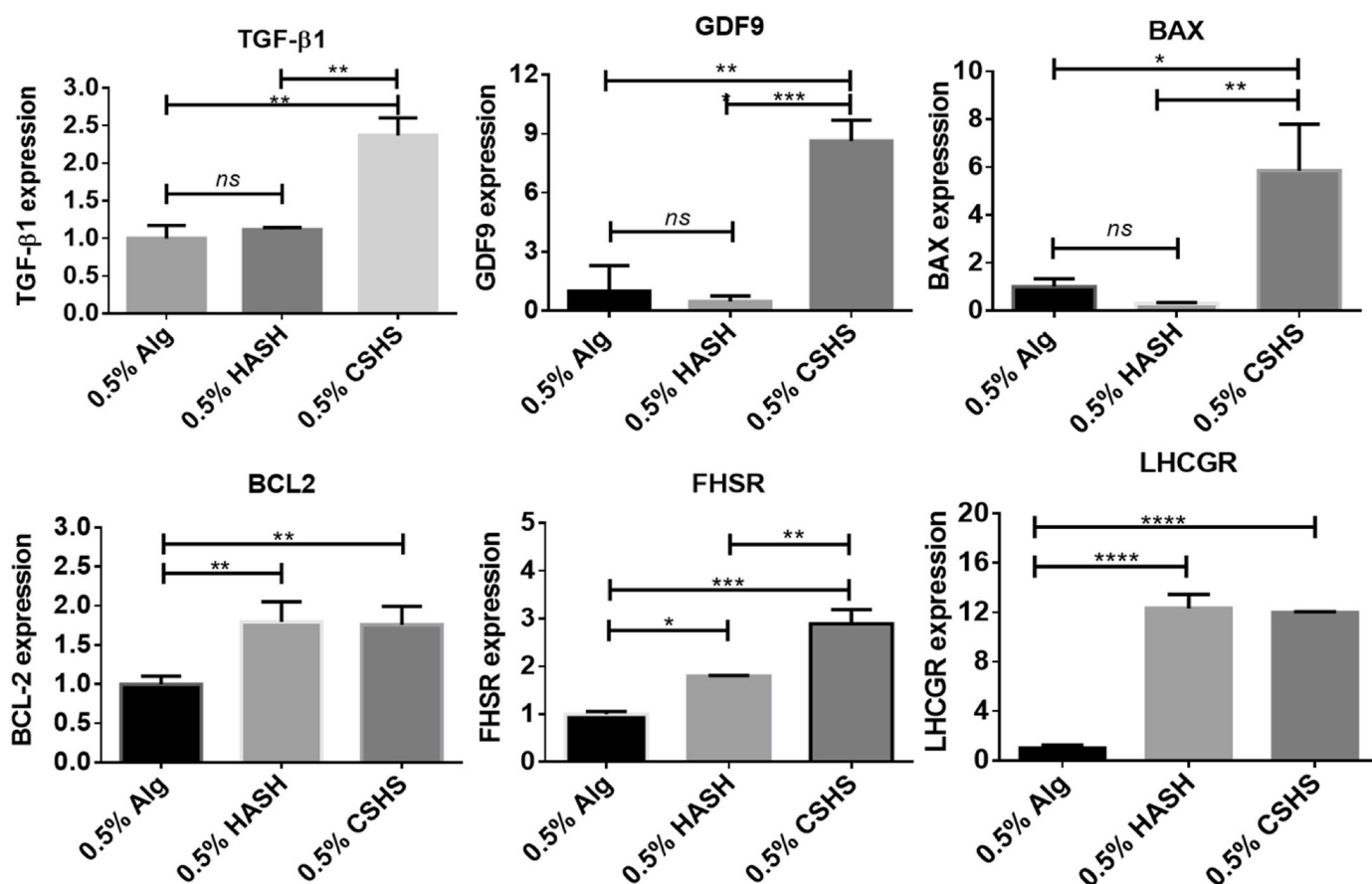


Fig. 8. Gene expression analysis of TGF- β 1, GDF9, BCL2, BAX, LHCGR and FSHR. Data are presented as mean \pm standard error (SE). Statistical analysis was performed by one-way analysis of variance (ANOVA) or Tukey's test. The results are expressed as the mean \pm standard deviation (SD; n = 4). *, $p < 0.05$; **, $p < 0.01$; ***, $p < 0.001$; ****, $p < 0.0001$. The data represent three separate experiments.

encapsulating mouse ovarian follicles in Alg has the potential to produce competent oocytes through *in vitro* follicle culture. Several studies have been combined natural polymer such as gelatin, HA, collagen, ECM to improve biological properties of Alg [58–60]. Recently, Zand et al. conducted Wharton's Jelly Hydrogel (WJH) composite of Alg hydrogel to improve biological properties of Alg [60]. However, WJH alone could not be used for bead construction since they were not solid enough for handling during transplantation. Laronda et al. and Wu et al. employed gelatin scaffold to provide a suitable environment for murine ovarian follicles culture [61,62]. HA has been widely employed to create 3D culture systems that mimic the *in vivo* microenvironment, facilitating stem cell growth and differentiation due to its ECM-like properties and biodegradability. Jamalzaei et al. reported that HA-encapsulated follicles exhibited higher GV to GVBD/MII rate transition, increased gene expression, and higher estradiol production than Alg and fibrin hydrogels [35,63]. CS-based hydrogels were employed for follicular growth and oocyte maturation. CS hydrogel showed higher survival rates, MII oocyte numbers, normal meiotic spindle appearance, and chromosome alignment [37].

Our research aimed to establish a 3D follicle culture platform using HA and CS-based materials due to their promising properties. HA is highly biocompatible and widely used in stem cell culture. CS has high biocompatibility and tunable mechanical properties which positively affects follicle development. To enhance the suitable biological and mechanical properties of materials for follicle culture, our culture system was developed by combining HA as the based material with CS to create the CSHS hydrogel through thiol-yne click crosslinking. Because of its naturally cationic amine of CS polymer, it has the potential to interact with an anionic HA chain to serve as the second crosslink

through electrostatic interaction and thereby enhancing mechanical properties. Moreover, mechanical strength of CSHS hydrogel could be modulated by altering the concentration and ratio of its two components during application. Interestingly, the follicles developed in this CSHS hydrogel culture system could be retrieved via mechanical isolation. This approach is designed to overcome the limitations associated with enzyme treatment, which can potentially harm the follicles and compromise their viability and functionality. By utilizing cost-effective HA and CS, and considering the advantages of the CSHS hydrogel that we have highlighted, we expected that our hydrogel could be an option for further exploration in the clinical applications for human follicle culture. To understand whether the proposed culture condition is ideal for follicle development, the morphological characteristics, diameter, survival rates of the cultured follicles, and meiotic resumption of their oocytes were assessed [64,65].

According to the physical characteristics of hydrogel described in previous section, we designed the study divided to 4 different crosslink hydrogels: Schiff-base:CHO-HA/Gel-NH₂ (Fig. S4), disulfide: HASH, thiol-yne: CSHS and ionic crosslink: Alg. However, culturing follicle in Schiff-base:CHO-HA/Gel-NH₂ hydrogel could not promote follicle growth and finally follicle degraded (Fig. S5). This study could be described that the culture of follicles in Schiff-base CHO-HA/Gel-NH₂ hydrogel did not result in follicle growth but rather led to follicle degradation. This highlights the importance of cautious reactant selection and formulation optimization to minimize cytotoxicity arising from aldehydes and amines. While Schiff-base hydrogels offer adjustable properties due to their dynamic nature, this characteristic can also influence stability, potentially causing premature degradation and loss of mechanical integrity. These findings underscore the requirement for

further research and development to address these limitations and refine the utilization of Schiff-base hydrogels in follicle culture.

Divalent cations of calcium (Ca^{2+}) are utilized to ionically crosslink Alg hydrogel. Moreover, isolated follicles have been cultured using Alg, with encouraging outcomes from various animal species. According to previous studies, the physical characteristics of Alg, which were controlled by its composition and concentration, had an impact on the development of antrums, maturation, as well as their expression of genes and hormonal secretions [56]. Previous studies showed that the Alg matrix varied from 0.125 to 3% concentrations were used for follicle encapsulation *in vitro*. It was shown that lower Alg concentrations were more favorable for mouse folliculogenesis [56,66,67]. The survival rate of the follicles incubated with 0.5% Alg was much greater than that with 0.75 and 1% Alg, and the results were generally similar to the study by Jamalzaei et al. [63]. It has been previously suggested that increasing the Alg concentration could limit follicles' access to hormones and other nutrients [54,68]. According to several studies of Alg, we designed to use 0.5% Alg hydrogel as a control group to compare follicle development *in vitro* with 0.5% HASH and 0.5% CSHS.

Each fully developed oocyte resumes maturation in the ovary in response to gonadotropins. This procedure prepares the oocyte ready for fertilization, sperm uptake, and the start of embryogenesis. In other words, oocyte maturation results in the generation of competent fertilizable oocytes. This process is completed after oocytes reach metaphase II (MII) stage. Oocytes are maturation incompetent and still arrested in the dictyate stage at the end of maturation, assigned as germinal vesicle (GV). When oocytes mature, the GV nuclear membrane breaks down, and they develop condensed chromosomes. This process is known as germinal vesicle breakdown (GVBD). Following the chromosomal arrangement in the MI stage, oocytes are arrested in MII. When they emit a polar body, these MII oocytes are prepared for fertilization [69]. According to our results, 0.5% CSHS and 0.5% HASH showed a greater proportion of GV and MII oocytes than 0.5% Alg. These findings had similar results reported by other researchers. HA and ECM-HA cultured follicles had similar survival rates, percent GVBD, and MII formation at the end of *in vitro* culture [34]. Another study by Parisa et al. employed a HAA hydrogel and OCs to culture mouse ovarian follicles compared with Alg and fibrin-alginate hydrogels [35]. Compared with Alg-developed oocytes, higher developed oocytes resumed meiosis up to the GVBD/MII stages in HAA ($P < 0.05$).

After oocyte maturation, the percentage of oocytes with an extruded first polar body is regularly utilized as a readout of oocyte meiotic competence. However, polar body extrusion is not a sufficient indicator of oocyte quality. To study the quality of the mature oocytes obtained following *in vitro* culture and had progressed to MII were analyzed for spindle integrity and chromosome alignment, two critical markers of oocyte developmental competence [70]. The chromosome assembly and normal morphologic spindle exhibit distinctive characteristics, such as chromosomes aligned on the equatorial plate and a barrel-shaped arrangement with slightly pointed poles produced by organized microtubules. Abnormal chromosome assembly and spindle configurations were observed including disorganization of microtubules, and chromosomes displaced from the spindle equatorial plane. These aberrant spindles or chromosomal alignments may have an impact on chromosome segregation, arrest maturation, or lead to the generation of aneuploidies [71,72]. Details of normal and abnormal patterns are given in Fig. 7.

According to the results, matured oocytes obtained from 0.5% Alg hydrogel exhibited the lowest normal spindle and chromosome alignment in our experiment, and similar results were reported by Mainigi et al. Isolated follicles that were encapsulated in 0.25% Alg had a higher incidence of spindle formation and chromosome alignment abnormalities as well as significant defects in cortical granule biogenesis [73]. Similarly, a recent study reported by P. Jamalzaei showed that both the absence and presence of OCs, the majority of 0.5% Alg developed oocytes did not show a consistent cortical distribution of cortical granules.

This examination is likely due to the clumping of cortical granules within the oocyte cytoplasm. Another critical factor might be because Alg does not have biological moiety to enhance proliferation and differentiation when encapsulating cells in hydrogels, thus resulting in the cause of poor oocyte development [74]. Meanwhile, a trend toward a higher incidence of spindle normality was found when oocytes were obtained from follicles cultured in 0.5% CSHS in our experiment. This finding is consistent with a previous study demonstrating that CS hydrogel was used to encapsulate follicles, compared with Alg hydrogel. The rate of the normal appearance of meiotic spindle, and chromosome alignment were higher in the CSHS group than those in the Alg group ($P \leq 0.05$).

The greater percentage of oocyte maturation and normal chromosome assembly and spindle configurations found in HA-based hydrogel (0.5% HASH and 0.5% CSHS) might be further described by the process of HA synthesis and its organization by cumulus cells. The presence of a HA matrix around the cumulus cells is most apparently responsible for the expansion of the preovulatory COC [75,76]. Thus, it might be concluded that using HA-based material could support oocyte maturation *in vitro*.

Regardless of the fact that 0.5% CSHS produced more mature MII oocytes with normal spindle organization and chromosomal alignment, the study's drawback was the lower amount of MII oocytes. To describe this limitation of this study, conditions that influence spindle organization and chromosomal alignment to *in vitro* matured oocytes have been reported. A previous study revealed that a low oxygen concentration and cooling and rewarming induced meiotic errors in the process of oocyte maturation *in vitro* [77]. Roberts et al. studied the chromosome alignment in mouse MI oocytes. They proposed that when MI oocytes reach the MII stage, FSH concentration influences chromosome orientation, increasing aneuploidy [78]. Moreover, Liu et al. also hypothesized that an increase in susceptibility to meiotic errors in early-stage follicles undergoing *in vitro* culture was probably related to the rate of chromosome aneuploidy in *in vitro* matured oocytes [79].

The expressions of some of the genes involved in growth and differentiation of follicles (TGF- β 1 and GDF9), steroidogenesis (FSHR and LHCGR), and apoptosis (BCL2 and BAX) were assessed in our study. TGF- β 1 is a potent factor for inducing HA synthesis by cumulus cells during the expansion of the COC and defining its independence from the oocyte factors. GDF9 is an oocyte-secreted protein that is present in all follicular stages and can promote follicular growth, differentiation, and expansion of cumulus cells and steroid metabolism in the ovary [80]. In the group with 0.5% CSHS, there was a high expression of GDF9, indicating effective communication between oocytes and granulosa cells. This enhanced communication potentially led to more pronounced follicle development, ultimately resulting in higher-quality fertilization and embryo development in this particular group. Apoptosis is a kind of programmed cell death, and has been associated with a range of processes that deal with normal functions of the follicular and ovary development, including atresia and corpus luteum regression. According to previous studies, COC with few markers of atresia has a higher potential for follicle development [81,82]. As such BCL2 increase, the oocyte may have a good development [83]. The overexpression of BAX in 0.5% CSHS could be described by the force exerted by the follicle and the stiffness of the hydrogel matrix. The apoptosis or lowered proliferation rates of follicular cells may be explained by the consequent increase in pressure on the follicle. This finding related to the slightly lower follicle survival rate in 0.5% CSHS. However, there was no significantly different in follicle viability compared with 0.5% Alg.

Ovarian granulosa (GCs) and theca cells (TCs) play essential regulatory roles in follicle development and oocyte maturation. FSH and LH are gonadotropins that signal through their cognate receptors. FSH acts through binding the FSHR expressed exclusively on GCs, whereas LH acts through binding the LHCGR expressed on both TCs and GCs [84]. The expression of FSHR in developing follicles is crucial for proper ovulation and fertility because the FSH-FSHR interaction stimulates a

series of intracellular signaling pathways that lead to the generation of steroid hormones, follicular maturation, and oogenesis. Furthermore, the FSHR gene can contribute to the increased production of estrogen hormones that promote the formation of GCs. Moreover, FSH could stimulate the transcription of the gene CYP19A1 in GCs, which transforms testosterone and other theca cell-derived androgens including dehydroepiandrosterone, androstenedione, androstenediol, into estrogens, estradiol, and estrone. LHCGR expression is a marker of follicle maturity throughout *in vitro* culture. In response to an increase in LH, the follicle may upregulate LHCGR, which would cause ovulation, granulosa cell luteinization, and cumulus mucification. This LHCGR data (Fig. 8) related to the results in Fig. 6 that HASH and CSHS could promote oocyte maturation.

When considering the differences between human and mouse folliculogenesis, several distinctions exist between the two species [85]. Folliculogenesis in mice progresses more rapidly than in humans, with a shorter duration from primordial to mature follicle stage. This results in mice reaching sexual maturity and reproductive capability much earlier in life compared to humans. Humans have a finite number of oocytes at birth, which steadily decreases over time, often depleting before menopause. Mice maintain a continuous supply of oocytes throughout their reproductive lives. However, the reproductive physiology of mice and humans differs, with mice having a shorter reproductive cycle and lifespan. Variations in hormonal regulation, such as estrogen and progesterone, exist between humans and mice, contributing to differences in follicular development and ovulation. Additionally, oocyte maturation occurs as part of the menstrual cycle in humans, whereas it is closely tied to the estrous cycle in mice. Additionally, human ovaries are larger and more robust than mouse ovaries, and tends to possess higher mechanical strength. An elastic modulus of less than 1 kPa has been observed in mice. However, considering the influence of matrix rigidity on human follicles, the preference leans towards stiffer biomaterials to facilitate optimal follicle growth. Considering the differences that we have highlighted in folliculogenesis between mice and humans, our CSHS hydrogel properties could serve as an alternative material for human follicle culture. This hydrogel is composed of natural polymers with exhibiting excellent biological properties. Notably, it obviates the need for enzyme treatment when isolating follicles from the hydrogel. Moreover, the mechanical strength could be adjusted by altering the concentration and composition ratio of the two polymer components, making it applicable to various animal species, including humans.

The field of *in vitro* follicle culture (IVC) is an active and evolving area of research with several future directions. The primary objective is to enhance follicle maturation *in vitro* by optimizing culture conditions and developing innovative systems that mimic the natural follicular environment. In humans, only a few ovarian follicles are found in the secondary stages, while the majority of follicles are primordial and located in the cortex. The primary objective of culturing primordial follicles is to preserve or enhance their developmental potential. This technique holds promise for applications in fertility preservation, *in vitro* maturation of oocytes for assisted reproductive technologies (ART), and research in the field of ovarian biology. It is important to note that *in vitro* culture of ovarian tissue pieces as a technique for *in situ* 3D follicle maturation has not proven to be highly effective. While it is possible to support the growth of primordial follicles using this approach, it inhibits the development of follicles beyond the pre-antral stage. Although most studies have been conducted growing follicles after the secondary follicle stage, only a limited number of studies have explored the culture of primordial follicles within ovarian cortex tissue [86–89].

Ongoing research also focuses on advancing biomaterials for IVC, including hydrogels, scaffolds, and 3D printing techniques, to create biomimetic microenvironments. Additionally, extending the duration of *in vitro* culture is a key goal to study follicle development over time and obtain mature and functional oocytes. Culturing primordial follicles is a complex and delicate process, with its success depends on various factors, including the quality of the ovarian tissue, the culture conditions,

and the specific objectives of the research or clinical application. Interestingly, early studies have demonstrated that the viability of primordial follicles isolated from thawed human ovarian cortical tissues was comparable to that of fresh tissue. However, a lower survival rate was observed in IVC of isolated primordial follicles [90,91]. Based on these findings, a consensus has been reached that the culture system based on primordial follicles should start from human ovarian cortex tissue rather than isolated primordial follicles [86,92–96]. Nonetheless, it holds the potential to advance our understanding of female reproductive biology and provide new possibilities for fertility preservation and infertility treatment.

The majority of *in vitro* culture studies of follicles typically focus on the preantral (secondary follicle) stage. Primordial follicles are abundant, and ideally, preserving and then culturing them would be the preferred approach. However, isolating and culturing them is exceptionally challenging due to their small size and limited granulosa cell layers, rendering them physically fragile. Therefore, a two-step method involving *in situ* tissue culture and subsequent follicle culture has been proposed. The optimization of *in vitro* culture techniques, including the use of biomaterials and the search for suitable materials, is primarily centered on the preantral stage follicles in existing research papers. In the human ovary, the largest number of follicles are primordial, and while it would be ideal to preserve them, technical limitations have led to research focusing on their isolation and preservation. The number of secondary follicles in a human ovary is significantly lower than that of primordial follicles. However, preserving and efficiently producing mature eggs from secondary follicles holds great clinical significance. The purpose of this study is to enhance the efficiency of preantral (secondary) follicle culture using novel materials. Given the relatively small number of secondary follicles, maximizing their development into mature eggs is importance. This is because it carries significant clinical implications for fertility preservation through *in vitro* follicle culture. Additionally, it is worth noting that research on the isolation and *in vitro* culture of primordial follicles is equally important and warrants further investigation.

Researchers have raised questions regarding the potential suitability of our hydrogel for primordial follicles and have requested further clarification on how these follicles can be cultured *in vitro* until they reach the secondary stage before being encapsulated in the hydrogel. As mentioned previously, numerous trials have been conducted to culture primordial follicles with tissue architecture. However, it is important to note that there is a significant lack of research in the field of bioengineering applied to ovarian tissue. Consequently, most researchers utilized work with growing follicles, including those in secondary stages, to produce competent oocytes for women who need to preserve their preservation.

The translation of IVC techniques into clinical applications, specifically for use in assisted reproductive technologies, requires further validation and refinement of protocols. Therefore, the hydrogel systems used in this study may serve as an alternate platform for future work on artificial fertility preservation.

5. Conclusions

In aspects of *in vitro* follicle growth and maturation, the ovarian follicle does not require vascularization because nutrients and waste products are carried through diffusion. Thus, the ability to present the appropriate combination of stimuli such as mechanical, diffusible and degradable during maturation is the only limitation to the development of an *in vitro* culture system. Our data indicated that thiol-yne crosslink CSHS hydrogel culture system was effective than other crosslink hydrogel types at supporting follicle growth, producing matured oocytes with greater number of normal spindle morphology and chromosome alignment. We believed that this platform could be applied as an alternative method to *in vitro* follicle culture with different experimental designs and clinical applications in the long-term period.

Statement of significance

A method that holds promise for maintaining female fertility is *in vitro* follicle culture. Additionally, using a 3D culture technique helps maintain the follicle's architecture and the maturation of the oocytes. To assess the impact of biomaterials on ovarian follicle development, CSHS hydrogel was developed. The spherical form of the follicle was maintained while encapsulating the follicle in CSHS hydrogel. Matured oocytes with normal appearance of meiotic spindle and chromosomal alignment were higher in the CSHS group compared with the Alg group. The expression level of folliculogenesis genes and endocrine-related genes was also higher in the CSHS group. These outcomes demonstrate that CSHS hydrogel is a permissive hydrogel and that it is advantageous for follicle development.

CRedit authorship contribution statement

Sureerat Khunmanee: Methodology, experiment conduction, Formal analysis, manuscript preparation. **Jungyoung Yoo:** Methodology, experiment conduction, Formal analysis, writing. **Jung Ryeol Lee:** Supervision, conception, Methodology. **Jaewang Lee:** Supervision, conception, Methodology. **Hansoo Park:** Supervision, conception, Methodology.

Declaration of competing interest

The authors declare that they have no known competing financial interests or personal relationships that could have appeared to influence the work reported in this paper.

Data availability

Data will be made available on request.

Acknowledgements

This research was supported by the National Research Foundation of Korea (NRF) funded by Ministry of Science and ICT (NRF-2021R1A2C2007189) and the Korea Health Technology R&D Project through the Korea Health Industry Development Institute (KHIDI), funded by the Ministry of Health and Welfare, Republic of Korea (HI14C3484 and HI21C1353).

Appendix A. Supplementary data

Supplementary data to this article can be found online at <https://doi.org/10.1016/j.mtbio.2023.100867>.

References

- C.-Y. Kuo, H. Baker, M.H. Fries, J.J. Yoo, P.C.W. Kim, J.P. Fisher, Bioengineering strategies to treat female infertility, *Tissue Eng., Part B* 23 (3) (2017) 294–306, <https://doi.org/10.1089/ten.teb.2016.0385>.
- A. Arav, P. Patrizio, Techniques of cryopreservation for ovarian tissue and whole ovary, *Clin. Med. Insights Reprod. Health* 13 (2019), <https://doi.org/10.1177/1179558119884945>, 1179558119884945–1179558119884945.
- E.C. Rivas Leonel, C.M. Lucci, C.A. Amorim, Cryopreservation of human ovarian tissue: a review, *Transfus. Med. Hemotherapy* 46 (3) (2019) 173–181, <https://doi.org/10.1159/000499054>.
- S.G. Kristensen, C.Y. Andersen, Cryopreservation of ovarian tissue: opportunities beyond fertility preservation and a positive view into the future, *Front. Endocrinol.* 9 (2018), <https://doi.org/10.3389/fendo.2018.00347>.
- S.Z. Sadr, B. Ebrahimi, M. Shahhoseini, R. Fatehi, R. Favaedi, Mouse preantral follicle development in two-dimensional and three-dimensional culture systems after ovarian tissue vitrification, *Eur. J. Obstet. Gynecol. Reprod. Biol.* 194 (2015) 206–211, <https://doi.org/10.1016/j.ejogrb.2015.09.028>.
- S. Joo, S.H. Oh, S. Sittadjody, E.C. Opara, J.D. Jackson, S.J. Lee, J.J. Yoo, A. Atala, The effect of collagen hydrogel on 3D culture of ovarian follicles, *Biomed. Mater.* 11 (6) (2016), 065009, <https://doi.org/10.1088/1748-6041/11/6/065009>.
- J.E. Swain, T.B. Pool, ART failure: oocyte contributions to unsuccessful fertilization, *Hum. Reprod. Update* 14 (5) (2008) 431–446, <https://doi.org/10.1093/humupd/dmn025>.
- M.W. Jurema, D. Nogueira, In vitro maturation of human oocytes for assisted reproduction, *Fertil. Steril.* 86 (5) (2006) 1277–1291, <https://doi.org/10.1016/j.fertnstert.2006.02.126>.
- Y. Wang, A. Anazodo, S. Logan, Systematic review of fertility preservation patient decision aids for cancer patients, *Psycho Oncol.* 28 (3) (2019) 459–467, <https://doi.org/10.1002/pon.4961>.
- D. Zhao, I.H. Leghari, J. Li, Y. Mi, C. Zhang, Isolation and culture of chicken growing follicles in 2- and 3-dimensional models, *Theriogenology* 111 (2018) 43–51, <https://doi.org/10.1016/j.theriogenology.2018.01.012>.
- M. Fujihara, T. Kaneko, M. Inoue-Murayama, Vitrification of canine ovarian tissues with polyvinylpyrrolidone preserves the survival and developmental capacity of primordial follicles, *Sci. Rep.* 9 (1) (2019) 3970, <https://doi.org/10.1038/s41598-019-40711-6>.
- J.B. Nagashima, D.E. Wildt, A.J. Travis, N. Songsasen, Activin promotes growth and antral cavity expansion in the dog ovarian follicle, *Theriogenology* 129 (2019) 168–177, <https://doi.org/10.1016/j.theriogenology.2019.02.018>.
- Q. Yang, L. Zhu, L. Jin, Human follicle in vitro culture including activation, growth, and maturation: a review of research progress, *Front. Endocrinol. (Lausanne)* 11 (2020) 548, <https://doi.org/10.3389/fendo.2020.00548>.
- V.R. Araújo, M.O. Gastal, J.R. Figueiredo, E.L. Gastal, In vitro culture of bovine preantral follicles: a review, *Reprod. Biol. Endocrinol.* 12 (2014) 78, <https://doi.org/10.1186/1477-7827-12-78>.
- J.I. Ahn, S.T. Lee, J.H. Park, J.Y. Kim, J.H. Park, J.K. Choi, G. Lee, E.S. Lee, J. M. Lim, In vitro-growth and gene expression of porcine preantral follicles retrieved by different protocols, *Asian-Australas. J. Anim. Sci.* 25 (7) (2012) 950–955, <https://doi.org/10.5713/ajas.2010.10355>.
- E. Galdones, L.D. Shea, T.K. Woodruff, in: B.R.M.B. Rizk, D.K. Gardner, T. Falcone (Eds.), *Three-dimensional in vitro ovarian follicle culture, Human Assisted Reproductive Technology: Future Trends in Laboratory and Clinical Practice*, Cambridge University Press, Cambridge, 2011, pp. 167–176.
- X. He, Microfluidic encapsulation of ovarian follicles for 3D culture, *Ann. Biomed. Eng.* 45 (7) (2017) 1676–1684, <https://doi.org/10.1007/s10439-017-1823-7>.
- Y. He, K. Meng, X. Wang, Z. Dong, Y. Zhang, F. Quan, Comparison of bovine small antral follicle development in two- and three-dimensional culture systems, *An. Acad. Bras. Cienc.* 92 (2020), <https://doi.org/10.1590/0001-3765202020180935>.
- V.R. Araújo, M.O. Gastal, A. Wischral, J.R. Figueiredo, E.L. Gastal, In vitro development of bovine secondary follicles in two- and three-dimensional culture systems using vascular endothelial growth factor, insulin-like growth factor-1, and growth hormone, *Theriogenology* 82 (9) (2014) 1246–1253, <https://doi.org/10.1016/j.theriogenology.2014.08.004>.
- A. Dadashzadeh, S. Moghassemi, A. Shavandi, C.A. Amorim, A review on biomaterials for ovarian tissue engineering, *Acta Biomater.* 135 (2021) 48–63, <https://doi.org/10.1016/j.actbio.2021.08.026>.
- J. Kim, A.S. Perez, J. Clafin, A. David, H. Zhou, A. Shikanov, Synthetic hydrogel supports the function and regeneration of artificial ovarian tissue in mice, *NPJ Regen. Med.* 1 (1) (2016), 16010, <https://doi.org/10.1038/nnpjregenmed.2016.10>.
- J.E. Ihm, S.T. Lee, D.K. Han, J.M. Lim, J.A. Hubbell, Murine ovarian follicle culture in PEG-hydrogel: effects of mechanical properties and the hormones FSH and LH on development, *Macromol. Res.* 23 (4) (2015) 377–386, <https://doi.org/10.1007/s13233-015-3045-x>.
- G. Liu, S. Li, J. Ren, C. Wang, Y. Zhang, X. Su, Y. Dai, Effect of animal-sourced bioactive peptides on the in vitro development of mouse preantral follicles, *J. Ovarian Res.* 13 (1) (2020) 108, <https://doi.org/10.1186/s13048-020-00695-8>.
- M. Rizwan, A.E.G. Baker, M.S. Shoichet, Designing hydrogels for 3D cell culture using dynamic covalent crosslinking, *Adv. Healthcare Mater.* 10 (12) (2021), 2100234, <https://doi.org/10.1002/adhm.202100234>.
- Y. Ren, H. Zhang, Y. Wang, B. Du, J. Yang, L. Liu, et al., Hyaluronic acid hydrogel with adjustable stiffness for mesenchymal stem cell 3D culture via related molecular mechanisms to maintain stemness and induce cartilage differentiation, *ACS Appl. Bio Mater.* 4 (3) (2021) 2601–2613, <https://doi.org/10.1021/acsbm.0c01591>.
- J.E. Park, J. Lee, S.T. Lee, E. Lee, In vitro maturation on ovarian granulosa cells encapsulated in agarose matrix improves developmental competence of porcine oocytes, *Theriogenology* 164 (2021) 42–50, <https://doi.org/10.1016/j.theriogenology.2021.01.008>.
- P.K. Kreeger, J.W. Deck, T.K. Woodruff, L.D. Shea, The in vitro regulation of ovarian follicle development using alginate-extracellular matrix gels, *Biomaterials* 27 (5) (2006) 714–723, <https://doi.org/10.1016/j.biomaterials.2005.06.016>.
- S.Z. Sadr, R. Fatehi, S. Maroufizadeh, C.A. Amorim, B. Ebrahimi, Utilizing fibrin-alginate and matrigel-alginate for mouse follicle development in three-dimensional culture systems, *Biopreserv. Biobanking* 16 (2) (2018) 120–127, <https://doi.org/10.1089/bio.2017.0087>.
- X. Zhang, L. Jiang, Y. Tian, Y. Xia, L. Yan, C. Wu, T. Zhang, J. Zhu, Establishment of in-vitro three dimensional rat follicle culture system and validation of the applicability as an in vitro female reproductive toxicity testing system, *In Vitro Toxicol.* 58 (2019) 161–169, <https://doi.org/10.1016/j.tiv.2019.03.019>.
- Z. Rajabi, H. Yazdekhasi, S.M.H. Noori Mugahi, M. Abbasi, S. Kazemnejad, A. Shirazi, M. Majidi, A.-H. Zarnani, Mouse preantral follicle growth in 3D co-culture system using human menstrual blood mesenchymal stem cell, *Reprod. Biol.* 18 (1) (2018) 122–131, <https://doi.org/10.1016/j.repbio.2018.02.001>.
- I. Noh, N. Kim, H.N. Tran, J. Lee, C. Lee, 3D printable hyaluronic acid-based hydrogel for its potential application as a bioink in tissue engineering, *Biomater. Res.* 23 (1) (2019) 3, <https://doi.org/10.1186/s40824-018-0152-8>.

- [32] B.C. Dash, K. Duan, H. Xing, T.R. Kyriakides, H.C. Hsia, An in situ collagen-HA hydrogel system promotes survival and preserves the proangiogenic secretion of hiPSC-derived vascular smooth muscle cells, *Biotechnol. Bioeng.* 117 (12) (2020) 3912–3923, <https://doi.org/10.1002/bit.27530>.
- [33] S. Tavana, M. Azarnia, M.R. Valojerdi, A. Shahverdi, Hyaluronic acid-based hydrogel scaffold without angiogenic growth factors enhances ovarian tissue function after autotransplantation in rats, *Biomater. Mater.* 11 (5) (2016), 055006, <https://doi.org/10.1088/1748-6041/11/5/055006>.
- [34] N. Desai, F. Abdelhafez, A. Calabro, T. Falcone, Three dimensional culture of fresh and vitrified mouse pre-antral follicles in a hyaluronan-based hydrogel: a preliminary investigation of a novel biomaterial for in vitro follicle maturation, *Reprod. Biol. Endocrinol.* 10 (1) (2012) 29, <https://doi.org/10.1186/1477-7827-10-29>.
- [35] P. Jamalzaei, M. Rezazadeh Valojerdi, L. Montazeri, H. Baharvand, Applicability of hyaluronic acid-alginate hydrogel and ovarian cells for in vitro development of mouse preantral follicles, *Cell J.* (2020) 49–60, <https://doi.org/10.22074/cellj.2020.6925>.
- [36] P. Domalik-Pyzik, J. Chlopek, K. Pieliuchowska, in: M.I.H. Mondal (Ed.), *Chitosan-based hydrogels: preparation, properties, and applications, Cellulose-Based Superabsorbent Hydrogels*, Springer International Publishing, Cham, 2019, pp. 1665–1693.
- [37] F. Hassani, B. Ebrahimi, A. Moini, A. Ghiaseddin, M. Bazrafkan, G.H. Hassanzadeh, M.R. Valojerdi, Chitosan hydrogel supports integrity of ovarian follicles during in vitro culture: a preliminary of a novel biomaterial for three dimensional culture of ovarian follicles, *Cell J.* 21 (4) (2020) 479–493, <https://doi.org/10.22074/cellj.2020.6393>.
- [38] R. Machín, J.R. Isasi, I. Vélaz, β -Cyclodextrin hydrogels as potential drug delivery systems, *Carbohydr. Polym.* 87 (3) (2012) 2024–2030, <https://doi.org/10.1016/j.carbpol.2011.10.024>.
- [39] N.S. Malik, M. Ahmad, M.U. Minhas, Cross-linked β -cyclodextrin and carboxymethyl cellulose hydrogels for controlled drug delivery of acyclovir, *PLoS One* 12 (2) (2017), e0172727, <https://doi.org/10.1371/journal.pone.0172727>.
- [40] S. Bian, M. He, J. Sui, H. Cai, Y. Sun, J. Liang, Y. Fan, X. Zhang, The self-crosslinking smart hyaluronic acid hydrogels as injectable three-dimensional scaffolds for cells culture, *Colloids Surf. B Biointerfaces* 140 (2016) 392–402, <https://doi.org/10.1016/j.colsurfb.2016.01.008>.
- [41] T.I. Zarebinski, N.J. Doty, I.E. Erickson, R. Srinivas, B.M. Wirostko, W.P. Tew, Thiolated hyaluronan-based hydrogels crosslinked using oxidized glutathione: an injectable matrix designed for ophthalmic applications, *Acta Biomater.* 10 (1) (2014) 94–103, <https://doi.org/10.1016/j.actbio.2013.09.029>.
- [42] A.B. Lowe, Thiol-yne 'click'/coupling chemistry and recent applications in polymer and materials synthesis and modification, *Polymer* 55 (22) (2014) 5517–5549, <https://doi.org/10.1016/j.polymer.2014.08.015>.
- [43] M.A. Filatov, Y.V. Khranova, M.L. Semenova, In Vitro mouse ovarian follicle growth and maturation in alginate hydrogel: current state of the art, *Acta Naturae* 7 (2) (2015) 48–56, <https://doi.org/10.32607/20758251-2015-7-2-48-56>.
- [44] C.A. Amorim, A. Van Langendonck, A. David, M.-M. Dolmans, J. Donnez, Survival of human pre-antral follicles after cryopreservation of ovarian tissue, follicular isolation and in vitro culture in a calcium alginate matrix, *Hum. Reprod.* 24 (1) (2008) 92–99, <https://doi.org/10.1093/humrep/den343>.
- [45] R.M. Skory, Y. Xu, L.D. Shea, T.K. Woodruff, Engineering the ovarian cycle using in vitro follicle culture, *Hum. Reprod.* 30 (6) (2015) 1386–1395, <https://doi.org/10.1093/humrep/dev052>.
- [46] I. Demeestere, A. Delbaere, C. Gervy, M. Van den Bergh, F. Devreker, Y. Englert, Effect of preantral follicle isolation technique on in-vitro follicular growth, oocyte maturation and embryo development in mice, *Hum. Reprod.* 17 (8) (2002) 2152–2159, <https://doi.org/10.1093/humrep/17.8.2152>.
- [47] H. Pazoki, H. Eimani, F. Farokhi, A. Shahverdi, R. Salman Yazdi, L.S. Tahaei, Comparing the growth and the development of mouse pre-antral follicle in medium with PL (Platelet Layset) and with FBS, *Middle East Fertil. Soc.* 20 (4) (2015) 231–236, <https://doi.org/10.1016/j.mefs.2015.01.006>.
- [48] W.D. Mahaud-Fernandez, W. Naushad, T.D. Panzner, A. Bashir, G. Lal, C. M. Okeoma, BST-2 promotes survival in circulation and pulmonary metastatic seeding of breast cancer cells, *Sci. Rep.* 8 (1) (2018), 17608, <https://doi.org/10.1038/s41598-018-35710-y>.
- [49] S. Zhang, Y. Wu, Y. Weng, Z. Xu, W. Chen, D. Zheng, W. Lin, J. Liu, Y. Zhou, In vitro growth of mouse preantral follicles under simulated microgravity, *J. Vis. Exp.* 130 (2017), e55641, <https://doi.org/10.3791/55641>.
- [50] F. Sun, I. Betzendahl, Y. Shen, R. Cortvrindt, J. Smitz, U. Eichenlaub-Ritter, Preantral follicle culture as a novel in vitro assay in reproductive toxicology testing in mammalian oocytes, *Mutagenesis* 19 (1) (2004) 13–25, <https://doi.org/10.1093/mutage/geg040>.
- [51] M. Fantauzzi, B. Elsener, D. Atzei, A. Rigoldi, A. Rossi, Exploiting XPS for the identification of sulfides and polysulfides, *RSC Adv.* 5 (93) (2015) 75953–75963, <https://doi.org/10.1039/C5RA14915K>.
- [52] S. Poveda-Reyes, V. Moulisová, E. Sanmartín-Masiá, L. Quintanilla, M. Salmerón-Sánchez, G. Gallego Ferrer, Gelatin-hyaluronic acid hydrogels with tuned stiffness to counterbalance cellular forces and promote cell differentiation, *Macromol. Biosci.* 16 (2016) 1311–1324, <https://doi.org/10.1002/mabi.201500469>.
- [53] S. Sakai, H. Ohi, M. Taya, Gelatin/hyaluronic acid content in hydrogels obtained through blue light-induced gelation affects hydrogel properties and adipose stem cell behaviors, *Biomolecules* 9 (8) (2019) 342, <https://doi.org/10.3390/biom9080342>.
- [54] M. Heise, R. Koepsel, A.J. Russell, E.A. McGee, Calcium alginate microencapsulation of ovarian follicles impacts FSH delivery and follicle morphology, *Reprod. Biol. Endocrinol.* 3 (1) (2005) 47, <https://doi.org/10.1186/1477-7827-3-47>.
- [55] E.J. Kim, C. Yang, J. Lee, H.W. Youm, J.R. Lee, C.S. Suh, S.H. Kim, The new biocompatible material for mouse ovarian follicle development in three-dimensional in vitro culture systems, *Theriogenology* 144 (2020) 33–40, <https://doi.org/10.1016/j.theriogenology.2019.12.009>.
- [56] E.R. West, M. Xu, T.K. Woodruff, L.D. Shea, Physical properties of alginate hydrogels and their effects on in vitro follicle development, *Biomaterials* 28 (30) (2007) 4439–4448, <https://doi.org/10.1016/j.biomaterials.2007.07.001>.
- [57] L. Liverani, N. Raffel, A. Fattahi, B. Beiki, V. Akbarinejad, C.A. Amorim, M. R. Valojerdi, L.A. Tahaei, R. Fathi, Successful 3D culture and transplantation of mouse isolated preantral follicles in hydrogel of bioengineered Johnston's jelly, *PLoS One* 18 (9) (2023), e0290095, <https://doi.org/10.1371/journal.pone.0290095>.
- [61] M.M. Laronda, A.L. Rutz, S. Xiao, K.A. Whelan, F.E. Duncan, E.W. Roth, T. K. Woodruff, R.N. Shah, A bioprosthetic ovary created using 3D printed microporous scaffolds restores ovarian function in sterilized mice, *Nat. Commun.* 8 (2017), 15261, <https://doi.org/10.1038/ncomms15261>.
- [62] T. Wu, Y.Y. Gao, J. Su, X.N. Tang, Q. Chen, L.W. Ma, J.J. Zhang, J.M. Wu, S. X. Wang, Three-dimensional bioprinting of artificial ovaries by an extrusion-based method using gelatin-methacryloyl bioink, *Climacteric* (2021) 1–9, <https://doi.org/10.1080/13697137.2021.1921726>.
- [63] P. Jamalzaei, M.R. Valojerdi, L. Montazeri, H. Baharvand, Effects of alginate concentration and ovarian cells on in vitro development of mouse preantral follicles: a factorial study, *Int. J. Fertil. Steril.* 13 (4) (2020) 330–338, <https://doi.org/10.22074/ijfs.2020.5746>.
- [64] C.A. Amorim, A. Shikanov, The artificial ovary: current status and future perspectives, *Future Oncol.* 12 (20) (2016) 2323–2332, <https://doi.org/10.2217/fon-2016-0202>.
- [65] M.C. Chiti, J. Donnez, C.A. Amorim, M.M. Dolmans, From isolation of human ovarian follicles to the artificial ovary: tips and tricks, *Minerva Ginecol.* 70 (4) (2018) 444–455, <https://doi.org/10.23736/s0026-4784.18.04231-4>.
- [66] E.R. West-Farrell, M. Xu, M.A. Gombert, Y.H. Chow, T.K. Woodruff, L.D. Shea, The mouse follicle microenvironment regulates antrum formation and steroid production: alterations in gene expression profiles, *Biol. Reprod.* 80 (3) (2009) 432–439.
- [67] M. Xu, E. West, L.D. Shea, T.K. Woodruff, Identification of a stage-specific permissive in vitro culture environment for follicle growth and oocyte development, *Biol. Reprod.* 75 (6) (2006) 916–923, <https://doi.org/10.1095/biolreprod.106.054833>.
- [68] Z.-X. Jiao, T.K. Woodruff, Follicle microenvironment-associated alterations in gene expression in the mouse oocyte and its polar body, *Fertil. Steril.* 99 (5) (2013) 1453–1459, <https://doi.org/10.1016/j.fertnstert.2012.12.009>.
- [69] Z.Q. Chen, T.X. Ming, H.I. Nielsen, Maturation arrest of human oocytes at germinal vesicle stage, *J. Hum. Reprod. Sci.* 3 (3) (2010) 153–157, <https://doi.org/10.4103/0974-1208.74161>.
- [70] S. Xiao, F.E. Duncan, L. Bai, C.T. Nguyen, L.D. Shea, T.K. Woodruff, Size-specific follicle selection improves mouse oocyte reproductive outcomes, *Reproduction* 150 (3) (2015) 183–192, <https://doi.org/10.1530/REP-15-0175>.
- [71] E. Vogt, M. Kirsch-Volders, J. Parry, U. Eichenlaub-Ritter, Spindle formation, chromosome segregation and the spindle checkpoint in mammalian oocytes and susceptibility to meiotic error, *Mutat. Res. Genet. Toxicol. Environ. Mutagen* 651 (1) (2008) 14–29, <https://doi.org/10.1016/j.mrgtox.2007.10.015>.
- [72] K.A. Campen, K.M. Kucharczyk, B. Bogin, J.M. Ehrlich, C.M.H. Combelles, Spindle abnormalities and chromosome misalignment in bovine oocytes after exposure to low doses of bisphenol A or bisphenol S, *Hum. Reprod.* 33 (5) (2018) 895–904, <https://doi.org/10.1093/humrep/dey050>.
- [73] M.A. Mainigi, T. Ord, R.M. Schultz, Meiotic and developmental competence in mice are compromised following follicle development in vitro using an alginate-based culture system, *Biol. Reprod.* 85 (2) (2011) 269–276, <https://doi.org/10.1095/biolreprod.111.091124>.
- [74] H. Cao, L. Duan, Y. Zhang, J. Cao, K. Zhang, Current hydrogel advances in physicochemical and biological response-driven biomedical application diversity, *Signal Transduct. Targeted Ther.* 6 (1) (2021) 426, <https://doi.org/10.1038/s41392-021-00830-x>.
- [75] N. Takahashi, W. Tarumi, B. Ishizuka, Involvement of hyaluronan synthesis in ovarian follicle growth in rats, *Reproduction* 147 (2) (2014) 189–197, <https://doi.org/10.1530/rep-13-0464>.
- [76] E. Suchanek, V. Simunic, D. Juretic, V. Grizelj, Follicular fluid contents of hyaluronic acid, follicle-stimulating hormone and steroids relative to the success of in vitro fertilization of human oocytes, *Fertil. Steril.* 62 (2) (1994) 347–352, [https://doi.org/10.1016/s0015-0282\(16\)56890-3](https://doi.org/10.1016/s0015-0282(16)56890-3).
- [77] R.R. Aman, J.E. Parks, Effects of cooling and rewarming on the meiotic spindle and chromosomes of in vitro-matured bovine oocytes, *Biol. Reprod.* 50 (1) (1994) 103–110, <https://doi.org/10.1095/biolreprod50.1.103>.
- [78] R. Roberts, A. Iatropoulou, D. Ciantar, J. Stark, D.L. Becker, S. Franks, K. Hardy, Follicle-stimulating hormone affects metaphase I chromosome alignment and

- increases aneuploidy in mouse oocytes matured in vitro, *Biol. Reprod.* 72 (1) (2005) 107–118, <https://doi.org/10.1095/biolreprod.104.032003>.
- [79] M. Conti, F. Franciosi, Acquisition of oocyte competence to develop as an embryo: integrated nuclear and cytoplasmic events, *Hum. Reprod. Update* 24 (3) (2018) 245–266, <https://doi.org/10.1093/humupd/dmx040>.
- [80] L.M. Gui, I.M. Joyce, RNA interference evidence that growth differentiation factor-9 mediates oocyte regulation of cumulus expansion in mice, *Biol. Reprod.* 72 (1) (2005) 195–199, <https://doi.org/10.1095/biolreprod.114.121368>.
- [81] S. Bilodeau-Goeseels, P. Panich, Effects of oocyte quality on development and transcriptional activity in early bovine embryos, *Anim. Reprod. Sci.* 71 (3) (2002) 143–155, [https://doi.org/10.1016/S0378-4320\(01\)00188-9](https://doi.org/10.1016/S0378-4320(01)00188-9).
- [82] P. Blondin, M.-A. Sirard, Oocyte and follicular morphology as determining characteristics for developmental competence in bovine oocytes, *Sci. Res.* 41 (1) (1995) 54–62, <https://doi.org/10.1002/mrd.1080410109>.
- [83] A. Ali, M.-A. Sirard, Effect of the absence or presence of various protein supplements on further development of bovine oocytes during in vitro maturation, *Biol. Reprod.* 66 (4) (2002) 901–905, <https://doi.org/10.1095/biolreprod66.4.901>.
- [84] K.C. Liu, W. Ge, Evidence for gating roles of protein kinase A and protein kinase C in estradiol-induced luteinizing hormone receptor (Lhcgr) expression in Zebrafish ovarian follicle cells, *PLoS One* 8 (5) (2013), e62524, <https://doi.org/10.1371/journal.pone.0062524>.
- [85] E. Gershon, N. Dekel, Newly identified regulators of ovarian folliculogenesis and ovulation, *Int. J. Mol. Sci.* 21 (12) (2020) 4565, <https://doi.org/10.3390/ijms21124565>.
- [86] O. Hovatta, C. Wright, T. Krausz, K.R.M. Hardy, Winston. Human primordial, primary and secondary ovarian follicles in long-term culture: effect of partial isolation, *Hum. Reprod.* 14 (10) (1999) 2519–2524, <https://doi.org/10.1093/humrep/14.10.2519>.
- [87] J. Li, K. Kawamura, Y. Cheng, A.J.W. Hsueh, Activation of dormant ovarian follicles to generate mature eggs, *Proc. Natl. Acad. Sci. USA* 107 (22) (2010) 10280–10284, <https://doi.org/10.1073/pnas.1001198107>.
- [88] E.E. Telfer, C.Y. Andersen, In vitro growth and maturation of primordial follicles and immature oocytes, *Fertil. Steril.* 115 (5) (2021) 1116–1125, <https://doi.org/10.1016/j.fertnstert.2021.03.004>.
- [89] V. Barbato, V. Genovese, V.D. Gregorio, M.D. Nardo, A. Travaglione, L.D. Napoli, G. Fragomeni, E.M. Zanetti, S.K. Adiga, G. Mondrone, T. D'Hooghe, W. Zheng, S. Longobardi, G. Catapano, R. Gualtieri, R. Talevi, Dynamic in vitro culture of bovine and human ovarian tissue enhances follicle progression and health, *Sci. Rep.* 13 (1) (2023), 11773, <https://doi.org/10.1038/s41598-023-37086-0>.
- [90] K. Oktay, D. Nugent, H. Newton, O. Salha, P. Chatterjee, R.G. Gosden, Isolation and characterization of primordial follicles from fresh and cryopreserved human ovarian tissue, *Fertil. Steril.* 67 (1997) 481–486, [https://doi.org/10.1016/S0015-0282\(97\)80073-8](https://doi.org/10.1016/S0015-0282(97)80073-8).
- [91] O. Hovatta, R. Silye, R. Abir, T. Krausz, R.M. Winston, Extracellular matrix improves survival of both stored and fresh human primordial and primary ovarian follicles in long-term culture, *Hum. Reprod.* 12 (5) (1997) 1032–1036, <https://doi.org/10.1093/humrep/12.5.1032>.
- [92] M. McLaughlin, D.F. Albertini, W.H.B. Wallace, R.A. Anderson, E.E. Telfer, Metaphase II oocytes from human unilaminar follicles grown in a multi-step culture system, *Mol. Hum. Reprod.* 24 (3) (2018) 135–142, <https://doi.org/10.1093/molehr/gay002>.
- [93] H.M. Picton, R.G. Gosden, In vitro growth of human primordial follicles from frozen-banked ovarian tissue, *Mol. Cell. Endocrinol.* 166 (1) (2000) 27–35, [https://doi.org/10.1016/S0303-7207\(00\)00294-X](https://doi.org/10.1016/S0303-7207(00)00294-X).
- [94] R.G. Gosden, J. Mullan, H.M. Picton, H.Y. S.-L. Tan, Current perspective on primordial follicle cryopreservation and culture for reproductive medicine, *Hum. Reprod. Update* 8 (2) (2002) 105–110, <https://doi.org/10.1093/humupd/8.2.105>.
- [95] R.A. Anderson, M. McLaughlin, W.H.B. Wallace, D.F. Albertini, E.E. Telfer, The immature human ovary shows loss of abnormal follicles and increasing follicle developmental competence through childhood and adolescence, *Hum. Reprod.* 29 (1) (2014) 97–106, <https://doi.org/10.1093/humrep/det388>.
- [96] Q. Yang, L. Zhu, L. Jin, Human follicle in vitro culture including activation, growth, and maturation: a review of research progress, *Front. Endocrinol.* 11 (2020) 548, <https://doi.org/10.3389/fendo.2020.00548>.